# Synthesis and Characterization of ZSM-5 Zeolite Membranes

Thesis by

Re Lai

In Partial Fulfillment of the Requirements

For the Degree of

Doctor of Philosophy

California Institute of Technology

Pasadena, California

2001

(Submitted July 24, 2000)

# Acknowledgements

It is with my deepest appreciation that I would like to thank my advisor, Professor George R. Gavalas, for mentoring me in the last five years. I have benefited tremendously from his guidance, thoughtful advice, and the extensive latitude allowed to me in the research.

I am deeply grateful to Professor Mark E. Davis and his group for their help and useful suggestions from time to time. I am also profoundly indebted to Professor Konstantinos P. Giapis for directing me to conduct experiments in his laboratory.

I wish to express my appreciation to the many people who helped me in many ways. In particular, I would like to acknowledge Piboon Pantu, Beom-Seok Kang, Yushan Yan, Shaocong Jiang, Huanting Wang, Neil Fernandes, Lixiong Zhang and Calum Chisholm. Special thanks to Dr. Chi Ma who assisted me in electron microscopy and X-ray diffraction experiments. Much gratitude to Weijun Zhou and Lin Luo for stimulating discussions. I would also like to thank Guy Duremberg of the machine shop and Rick Gerhart of the glass shop for putting up with my numerous ASAP requests.

Most of all, this work would not have been possible without the unconditioned support of my parents.

# Abstract

Synthesis of ZSM-5 zeolite membranes supported on porous alumina substrates was conducted in autoclave reactors. The film morphologies and structures were characterized by scanning electron microscopy, energy dispersive spectroscopy and X-ray diffraction. Gas adsorption was used to estimate the crystalline fraction of the products. The gas permeation properties of the membranes were evaluated for $H_2$, $CH_4$, $O_2$, $N_2$, and *n*-butane and other gases singly or in mixtures.

ZSM-5 film formation on alumina and other surfaces in certain clear, tetrapropylammonium($TPA^+$)-containing synthesis solutions was found to be preceded by a gel layer. The presence of alumina and other substrates of a high Hamaker constant facilitated formation of the surface gel layer and accelerated zeolite crystallization. Aluminum added to the solution or leached from alumina substrates had dual effects, to induce surface gelation and to retard crystallization of that layer as well as crystallization in the bulk solution.

Growth of ZSM-5 membranes was facilitated by using alumina tubes pre-coated with silicalite seeds. Accompanied with gradual growth of an external polycrystalline layer, siliceous deposits accumulated as deep as 100 μm inside the pores of the support, converting gradually from amorphous to crystalline. Pure gas permeation results are presented for membranes prepared in a solution of composition $SiO_2$: 0.15TPABr: 0.7NaOH: $98H_2O$ using 0.4 and 2 μm seeds.

Organic-free hydrogel reaction mixtures were further used to grow ZSM-5 membranes on seeded porous alumina substrates, eliminating the crack-prone calcination step for removing organic $TPA^+$ templates from as-synthesized ZSM-5. The optimum composition $SiO_2$: $0.0125Al_2O_3$: $0.2675Na_2O$: $46H_2O$ was identified to produce membranes with permeation selectivities for $H_2$ over *n*-butane above $10^4$ and for $O_2$ over $N_2$ 9-10. The permeation was strongly activated with the activation energies increasing sharply with molecular size.

Parallel synthesis of zeolite films was developed to expedite composition screening. The films prepared in an array reactor of multiple wells each containing 35 micro-liter synthesis solution displayed morphology similar to that produced by the conventional synthesis. The method was applied to explore the composition space of clear, organic-free synthesis solutions for ZSM-5 films growth: $SiO_2$: (700-300)$Al_2O_3$: (0.5-0.7)NaOH: $80H_2O$.

# Table of Contents

# List of Tables

# List of Figures

**Chapter 1**

# Introduction

## 1.1 Membrane Separation Processes

Separation processes are ubiquitous in the chemical industry accounting for 40-70% of capital and operating costs. Above 90% of all separations in chemical industry are conducted by distillation, an energy and capital intensive process that consumes $10 billion of energy per year in the United States [1,2]. Membrane separations offer a green alternative that is both energy efficient and convenient to operate, spurring strong academic and commercial interest. The worldwide membrane market reached $4 billon in 1996 [1]. The U.S. sales of membrane materials exceeded $1 billion in 1997, and the demand continues to grow steadily at 8.2% annually [3].

Membrane technologies are very diverse, encompassing a wide spectrum of applications ranging from the traditional filtration and reverse osmosis to the fast growing areas of molecular separation such as gas separation and pervaporation. The last 50 years witnessed the introduction of large-scale molecular separation membrane systems such as isotope separation, seawater desalination, and the Prism polysulfone hollow fiber applied to refining applications. Almost all commercial membranes used today for molecular separations are made of polymers. Polymeric membranes are relatively easy to fabricate into hollow fiber or spiral-wound configurations that provide large surface areas, but have certain drawbacks such as limited operational temperatures and vulnerability to organic swelling and fouling [4,5]. Inorganic membranes, on the other hand, offer attractive thermal stability, erosion resistance and durability that is not available to polymeric materials [6,7]. In selected separations they provide high selectivity

unattainable with polymeric membranes. Today, the inorganic membrane materials represent the fastest growing segment of the membrane market. At an impressive 20% annual growth rate, inorganic materials are poised to capture 15% of the membrane market in 2003 [7]. While water treatment continues to be the largest application for inorganic membranes, they have been increasingly deployed in other processes.

Inorganic membranes for gas separation can be classified into dense and porous. Palladium, silica and perovskite membranes are representative dense inorganic membranes used for $H_2$ or $O_2$ separation, in which the permeating molecules form interstitial species that diffuse through the membrane [7]. Dense membranes can offer high selectivities, but are limited to a few only separations and generally require elevated operating temperature. Porous inorganic membranes separate gases by Knudsen diffusion, surface diffusion or molecular sieving [6,7]. Mesoporous membranes (pore width about 2-50 nm) operate in the regime of combined Knudsen diffusion and surface diffusion, differentiating gas molecules by their molecular weights and adsorption property respectively, but the selectivity is usually not sufficient for commercial applications. Microporous membranes with pore size less than 1 nm can offer a strong interaction of the pore structure with diffusing molecules. This mechanism dictates that a uniform and narrow pore size distribution is desired for effective gas separation. The microporous inorganic membranes that are currently under active development include amorphous oxides made by the sol-gel or CVD process, porous carbon, and zeolites [7]. As porous oxides and carbon membranes are amorphous, controlled formation of narrow pore size distribution in them is quite challenging.

## 1.2 Zeolite Membranes

Zeolites include a diverse family of crystalline porous alumosilicates with a uniform and tunable cagelike structure [8,9]. There are about 100 types of synthetic and nature zeolites, with pore diameters generally falling into the sub-nanometer micropore range that is comparable to molecular sizes. They are stable at elevated temperature or under harsh chemical environments, and are widely utilized as molecular sieves in selective adsorption and shape-selective catalysis.

Zeolite MFI, including ZSM-5 and its alumina-free analogue, silicalite, is a class that has been extensively used in petrochemical industry as adsorbents and catalysts. ZSM-5 has a $SiO_2/Al_2O_3$ ratio of 20-500, while silicalite by definition has a $SiO_2/Al_2O_3$ ratio larger than 500. Zeolite ZSM-5 has two sets of intersecting 10-member oxygen channels of diameter *ca.* 0.55 nm, one straight and one sinusoidal. Zeolite MFI is generally prepared under hydrothermal conditions from an aqueous mixture containing silicate, aluminate, hydroxide and tetrapropylammonium ($TPA^+$). The $TPA^+$ cations, serving as a structure-directing agent, are encapsulated inside the as-synthesized zeolite powder and need to be removed by calcination in air at 400-500°C to make the zeolitic pores accessible.

While the stability and pore size uniformity make zeolites a desirable membrane separation material, the synthesis of such zeolite membranes has presented considerable difficulties. Such membranes must be made of a continuous film of micrometer-sized zeolite crystallites interlocking into each other in a manner that must exclude non-zeolitic

pathways. Furthermore, the membranes need to be supported on porous substrates to have sufficient mechanic strength.

Reasonably selective zeolite membranes were only achieved about ten years ago. Since then the number of publications has grown exponentially (Fig. 1). The majority of the publications deal with ZSM-5 and silicalite, and the membranes were found to have impressive separation properties for hydrocarbons and water-organic mixtures [10-17]. Other types of zeolite membranes such as A-type and X,Y-type have also been reported [18-20]. While the primary motivation for zeolite film synthesis is for separation applications, supported zeolite films are also being pursued for applications in the fields of nonlinear optic materials, catalytic membrane reactors and gas sensors [21,22].

The objective of this Ph.D. research was to advance zeolite membrane synthesis with focus on designing novel synthesis approaches with dual goals, to improve the robustness of the synthesis procedure and to obtain membranes of better performance. Meanwhile, as zeolite membrane growth is far from well understood, part of the effort was devoted to a better understanding of zeolite membrane growth on porous substrates.

## 1.3 Outline

While zeolite crystallization has been the subject of intense study (see, e.g., [23,24]), much still remains unclear because of the complex interactions of monomeric, oligomeric, and polymeric aluminosilicates, organic structural-directing agents, hydroxide ions, cations, and solvents during the hydrothermal reaction. Zeolite film

growth on a substrate adds another level of complexity as a result of the interplay of the substrate and the reaction mixture, and little is thus known about zeolite film formation. **Chapter 2** investigates the ZSM-5 zeolite film growth on alumina and other surfaces, with a main focus on the effects of substrate and aluminum in solution on surface gelation and crystallization. ZSM-5 film growth was found to start with a surface gel layer, whose formation was facilitated by the presence of substrates having a high Hamaker constant. Aluminate ions added to the solution or leached from alumina substrates had dual effects, to induce a gel layer to form on the substrate surface and to impede zeolite crystallization. The study concludes that zeolite film growth is possible only in a limited window of opportunity.

**Chapter 3** presents a method to relieve the stringent requirements on synthesis conditions for successful membrane growth by using substrates pre-coated with a closely packed layer of zeolite seed particles. Effective seeding on alumina substrates was carried out by simple immersion of the substrate in a silicalite suspension maintained at pH 8, intermediate between the isoelectric points (IEP's) of the support and silicalite. Surface seeding entails a high number of nuclei anchored at the surface, eliminating the necessity of surface nucleation. It also allows zeolite layer growth to proceed at lower temperature or shorter times than required when using unseeded supports.

**Chapter 4** further extends the surface seeding method to $TPA^+$-free synthesis. The synthesis protocol used to date for ZSM-5 membranes have invariably employed organic $TPA^+$ cations to direct the crystallization, producing as-synthesized zeolite with encapsulated $TPA^+$ that must be removed to access the pores. During calcination $TPA^+$

decomposition results in an abrupt shrinkage of the zeolite lattice that tends to produce micro-cracks in the zeolite layer. Adoption of $TPA^+$-free synthesis of ZSM-5 renders calcination unnecessary, but also makes the crystallization field much narrower. This study used surface seeding to help extend the composition space for successful membrane growth in the absence of organic $TPA^+$ cations, and an organic-free hydrogel composition was identified to yield highly permselective ZSM-5 membranes.

**Chapter 5** introduces parallel synthesis to facilitate composition screening for zeolite film preparation. The technique is applied to explore the composition space of clear, organic-free synthesis solutions for ZSM-5 films. Previous organic-free synthesis of ZSM-5 in either powder or film form invariably employed hydrogel reaction mixtures. Clear solution synthesis of ZSM-5 powders has been quite popular in crystallization mechanism investigation as it allows direct observation of the crystallization process and easy product separation. Clear solutions are also desirable in film preparation to prevent spatial inhomogeneities. Thus, this study, after examining some operational details, illustrates parallel synthesis of ZSM-5 films from clear, organic-free solutions.

## References

[1] Humphrey, J.L.; Keller II, G.E. *Separation Process Technology*; McGraw-Hill: New York, 1997.

[2] Seader, J.D.; Henley, E.J. *Separation Process Principles*; John Wiley & Sons: New York, 1998.

[3] Fredonia Group, *Membrane Separation Technologies to 2002*; Fredonia Group: Cleveland, 1998.

[4] Osada, Y.; Nakagawa, T. *Membrane Science and Technology*; Marcel Dekker: New York, 1992.

[5] Kesting, R.E.; Fritzsche, A.K. *Polymeric Gas Separation Membranes*; John Wiley & sons: New York, 1993.

[6] Bhave, R.R. *Inorganic Membrane Synthesis, Characteristics and Applications*; Van Nostrand Reinhold: New York, 1991.

[7] Burggraaf, A.J.; Cot, L. *Fundamentals of Inorganic Membrane Science and Technology*; Elsevier: Amsterdam, 1996.

[8] Breck, D.W. *Zeolite Molecular Sieves*; Robert E Kreiger Publishing Company: Malabar, Florida, 1984.

[9] Szostak, R. *Molecular Sieves: Principles of Synthesis and Identifications*; 2nd ed.; Van Nostrand Reinhold: New York, 1998.

[10] Geus, E.R.; den Exter, M.J.; van Bekkum, H. *J. Chem. Soc.-Faraday Trans.* **1992**, *88*, 3101.

[11] Jia, M.D.; Chen, B.S.; Noble, R.D.; Falconer, J.L. *J. Membr. Sci.* **1994**, *90*, 1.

[12] Yan, Y.S.; Davis, M.E.; Gavalas, G.R. *Ind. Eng. Chem. Res.* **1995**, *34*, 1652.

[13] Vroon, Z.; Keizer, K.; Gilde, M.J.; Verweij, H.; Burggraaf, A.J. *J. Membr. Sci.* **1996**, *113*, 293.

[14] Bakker, W.J.W.; Kapteijn, F.; Poppe, J.; Moulijn, J.A. *J. Membr. Sci.* **1996**, *117*, 57.

[15] Kusakabe, K.; Yoneshige, S.; Murata, A.; Morooka, S. *J. Membr. Sci.* **1996**, *116*, 39.

[16] Lovallo, M.C.; Tsapatsis, M. *AICHE J.* **1996**, *42*, 3020.

[17] Coronas, J.; Falconer, J.L.; Noble, R.D. *AICHE J.* **1997**, *43*, 1797.

[18] Boudreau, L.C.; Tsapatsis, M. *Chem. Mat.* **1997**, *9*, 1705.

[19] Matsufuji, T.; Nishiyama, N.; Ueyama, K.; Matsukata, M. *Microporous Mesoporous Mat.* **1999**, *32*, 159.

[20] Nishiyama, N.; Matsufuji, T.; Ueyama, K.; Matsukata, M. *Microporous Mater.* **1997**, *12*, 293.

[21] Koegler, J.H.; Zandbergen, H.W.; Harteveld, J.L.N.; Nieuwenhuizen, M.S.; Jansen, J.C.; van Bekkum, H. *Stud. Surf. Sci. Catal.* **1994**, *84*, 307.

[22] Bein, T. *Chem. Mat.* **1996**, *8*, 1636.

[23] Burkett, S.L.; Davis, M.E. *J. Phys. Chem.* **1994**, *98*, 4647.

[24] Davis, M.E.; Zones, S.I. In *Synthesis of Porous Materials: Zeolites, Clays, and Nanostructures*, Occelli, M.L. and Kessler, H., Ed.; Marcel Dekker: New York, 1997; p. 1.

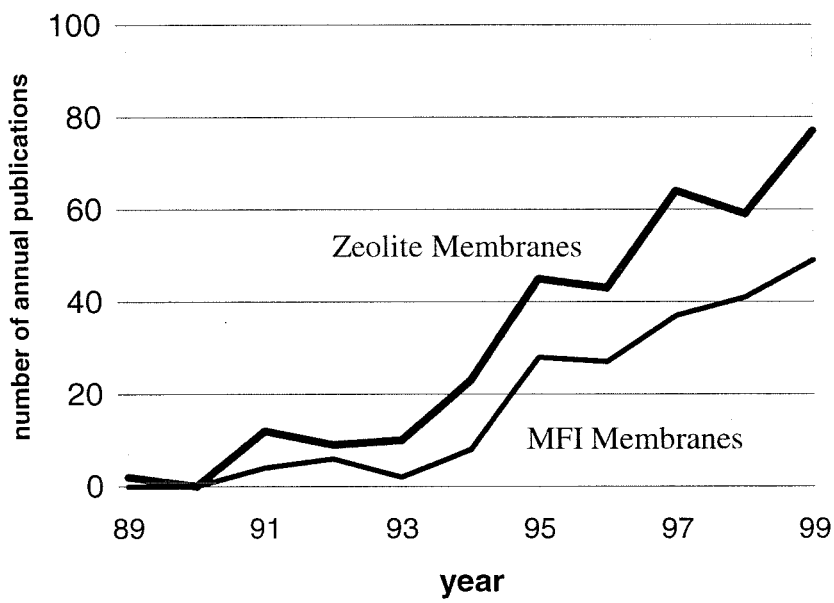


**Figure 1-1** The number of annual publications in zeolite membranes and MFI membranes. (Source: Scientific Citation Index)

**Chapter 2**

# Growth of ZSM-5 Films on Alumina and Other Surfaces

Reprinted from *Microporous and Mesoporous Materials*, 37 (2000) 9-19

# Growth of ZSM-5 Films on Alumina and Other Surfaces

Re Lai, Yushan Yan and George R. Gavalas

*Division of Chemistry and Chemical Engineering, California Institute of Technology*

*Pasadena, California 91125*

## Abstract

Growth of ZSM-5 films on porous α-Al2O3 and other substrates was studied with main focus on the effect of the substrate on surface gel formation and zeolitization. The films formed on the substrate and the powders that settled at the bottom of the autoclave were characterized by SEM and XRD. Adsorption of Ar and *iso*-butane was used to estimate the crystalline fraction of the product formed on and in the pores of the substrate. The presence of alumina substrates accelerated bulk zeolitization for certain solution compositions. Aluminum added to the solution had dual effects, to induce gel layer formation on the substrate surface and to retard zeolitization of that layer as well as retard zeolitization in the bulk of the solution.

## 2.1 Introduction

Growth of zeolite films on surfaces has been investigated from the standpoint of fundamental growth mechanisms and relative to the development of sensors, optoelectronic devices, and separation membranes. Except in membrane preparation, film

growth has been studied on smooth supports like silicon or polished metals. In membrane preparation, on the other hand, the substrates are porous and have a certain intrinsic roughness that cannot be eliminated by polishing. In this paper we report results concerning growth of ZSM-5 films obtained in the course of making supported zeolite membranes. The focus of this paper will be on the effect of aluminum content of the solution and the role of the alumina support on film and bulk zeolitization.

Zeolite membranes have been synthesized by a variety of approaches.[1-15] For certain synthesis compositions membrane growth on porous supports takes place from a clear solution so that nucleation at the support surface and subsequent growth into a continuous, defect-free film are essential for the preparation of selective membranes. Usually, the first step in membrane growth is the formation of a gel layer that serves as the primary source of nuclei and nutrient.[1,3,16-18] When surface seeding is used, nucleation is not anymore necessary,[6,19-22] but the gel layer can still have an important effect on membrane morphology.[9]

Zeolite film growth is still not fully understood but is known to involve complex interaction between the reaction mixture and the support. Delft researchers have proposed a mechanism emphasizing the adsorption and decomposition of $TPA^+$ (tetrapropyl ammonium) on silica surfaces in aluminum-free, $TPA^+$-monocationic systems.[23-27] Under alkaline reaction conditions, the negatively charged silica surface attracts $TPA^+$, which is subsequently decomposed by Hofmann degradation causing a more pronounced decline of pH in the vicinity of the surface than in the bulk. The $TPA^+$-deficient gel layer subsequently undergoes zeolitization at the gel-liquid interface.

The situation is more complicated if inorganic ions like $Na^+$ and aluminate are also present in the reaction mixture. Both are capable of promoting gelation, and $Na^+$ can compete against $TPA^+$ in surface adsorption. Experiments show that the morphology of zeolite films changes profoundly when $Na^+$ ions are incorporated.[3,18,24] In addition, substrates play a more active role than just to provide a negatively charged surface to anchor cations. Formation of a continuous film depends on the composition and pretreatment of supports[1,28,29] and their location in the reaction vessel.[12,30] This study examines in particular the multifaceted role of alumina supports in surface gel formation and subsequent zeolitization.

## 2.2 Experimental

The supports used in most experiments were $\alpha$-$Al_2O_3$ tubes (99.6%, Golden Technologies) of 9-10 mm o.d., 6-7 mm i.d., 0.2 μm mean pore diameter, and ca. 30% void fraction. Before use, the tubes were polished, ultrasonicated in water for 30 min., extracted by acetone in a Soxhlet extractor for 1 day, and dried at 105°C. Other supports used were thin non-porous alumina plates (99.8% $\alpha$-$Al_2O_3$) and zirconia plates ($ZrO_2$ 94 wt.%, $Y_2O_3$ 5.4 wt.%) from Intertec Southwest LLC, and fused-quartz disks (General Electric). Nonporous supports were ultrasonicated in acetone for 10 min., and further cleaned with an oxidizing solution of 70 vol% $H_2O$, 15 vol% $H_2O_2$ (30%) and 15 vol% $NH_3$ (25%) at 80°C for 10 min.[31]

The synthesis mixture was prepared by adding under stirring tetraethyl orthosilicate (TEOS) to an aqueous solution of NaOH, TPAOH, and aluminate followed by aging for 24 h at room temperature under stirring. The substrate was placed in a Teflon-lined stainless steel autoclave and held horizontally or vertically in the solution by a Teflon-holder. The horizontally positioned tubes were *ca.* 1 mm below the solution-air interface. The inside of the tubes was covered with Teflon tape so that films grew only at the outer surface. Non-porous plates were held horizontally at the top portion of the solution, *ca.* 1mm below the solution-air interface unless specified otherwise. The hydrothermal reaction was carried out in a forced-convection oven preheated at the reaction temperature. The films were calcined in a stream of oxygen at 400°C for 20 h at 1°C/min and subsequently cooled at the same rate.

The morphology of the films was examined by SEM (Camscan, 15 kv) and the phase of the zeolite was confirmed by XRD (Cu-$K_\alpha$). High resolution gas adsorption of uncalcined and calcined samples was conducted with an ASAP 2010 system (Micromeritics). Before adsorption, the uncalcined and calcined samples were degassed overnight at 180°C and 350°C respectively.

## 2.3 Results and discussion

### *Film evolution with reaction time*

A clear solution of composition $6SiO_2$- TPAOH- 4NaOH- $571H_2O$ was used for this series of experiments. This composition was similar to the one used earlier by Yan et al.,[3] except that it did not contain aluminum. SEM micrographs of the films formed after 8, 12 and 16 h reaction are shown in Fig. 1. The micrographs indicate that film growth starts with the formation of a gel layer. Zeolitization starts inside that layer and gradually transforms it into a zeolite film. For both horizontal and vertical orientation of the tubular substrates the zeolite film was intergrown and appeared continuous at the SEM magnification. Single gas permeation experiments showed that the films obtained after 16 h reaction have selective permeation properties, with single gas selectivities of *n*-butane over *iso*-butane to be 10-90.

The growth pattern in the films shown in Fig.1 differs from that observed in previous studies using aluminum-free, $TPA^+$-monocation systems where nucleation and crystallization were localized at the gel-liquid interface.[23-27] The different site of nucleation is not surprising because the solution used in the present work has higher alkalinity and contains $Na^+$ ions competing with $TPA^+$ for adsorption at the substrate surface.[18] Moreover, the substrate employed in the previous studies (refs. 23-27) was silicon rather than alumina as employed here. Recently, Nakazawa et al. using a composition similar to the one used here observed zeolite crystals growing within gel layers formed on quartz substrates.[18]

SEM of cross sections of films prepared as described above shows random intergrowth, different in morphology from the columnar feature of films prepared by surface seeding.[20-22] The columnar morphology in seeded synthesis results from competitive development of the fastest growing axis, which usually yields films with the *c*-axis of crystallites preferentially normal to the substrate surface. Under the reaction conditions used in the present study, crystallization and growth take place inside the gel layer, resulting in a randomly oriented polycrystalline film.

***Effects of aluminum in solution***

Films produced after 16 h of reaction in solutions of different Si/Al ratios are shown in Fig. 2. It is immediately obvious that increasing the aluminum content hinders zeolitization. For a reaction mixture with Si/Al<600, a continuous gel layer with no indication of crystallinity can be observed at 16 h. At Si/Al levels above 600, some zeolite particles are observed embedded in the gel layer. For an aluminum-free solution the film was fully crystallized in 16 h of reaction. The composition Si/Al=600 yielded a completely crystallized zeolite film when the reaction time was increased from 16 to 36 h, but even after 40 h the substrate placed in a solution with Si/Al=300 was still covered by a gel layer. All Si/Al ratios listed above refer to the solution before hydrothermal reaction. Aluminum leaching from the support would decrease that ratio especially near the support surface and further inside the pores. The extent of this leaching depends on the texture of the substrate. For example, $\alpha$-$Al_2O_3$ plates of 0.5 μm pore diameter developed fully crystalline films in 16 h in a solution of Si/Al ratio of 600 as compared to

the 36 h required by the tubular substrates (0.2 μm pore diameter) under the same conditions.

Hydrothermal synthesis conducted in the absence of supports but under otherwise similar conditions demonstrated the inhibition of bulk zeolite crystallization by aluminum. For a synthesis solution of Si/Al=600, as shown in Fig. 3, only amorphous particles (0.06 g) were formed after 16 h reaction at 175°C. After 48 h reaction, the precipitates (0.1 g) still remained largely amorphous, but crystallites began to form within the gel similar to the growth in the films shown in Fig. 1. After 90 h reaction, all precipitates (0.86 g) turned crystalline ZSM-5. By contrast, the precipitate (0.3 g) was zeolitic after only 16 h reaction at 175°C for a reaction mixture containing no aluminum.

It is well documented in the literature that increasing the content of aluminum in the synthesis solution suppresses zeolitization.[32-35] Golemme et al. concluded that aluminum decreases the nucleation rate,[36] while Persson et al. found that at low levels (Si/Al>100) aluminum suppresses nucleation but at higher levels it retards both nucleation and linear growth.[37] The decrease of the growth rate with the addition of aluminum was found most pronounced in the (001) direction.[36,38] Derouane et al. suggested that the difficulty to incorporate aluminum arises from the necessity to include exchange cations simultaneously with aluminum in the zeolite framework.[39]

EDS was used to estimate the Si/Al ratio and sodium content of films grown in solutions of different Si/Al ratios with the results listed in Table 1. The Si/Al ratio in the film increases with the ratio in the solution but in all cases it is much lower than the

latter. Although aluminum enrichment also takes place in bulk synthesis, in supported synthesis it is accentuated by aluminum leaching from the substrate. The effect of leaching is evident by referring to the film with Si/Al=225 grown in an aluminum-free solution. Enrichment of the aluminum content in ZSM-5 crystallized from clear synthesis solutions has been well documented[40,41] and generally attributed to the lower solubility of aluminate.[35] However, formation of ZSM-5 with a Si/Al ratio similar to that of the bulk clear solution was observed at high alkalinity and $TPA^+$ concentration that favor dissolution of aluminosilicates.[37,42]

To further study the effect of aluminum on film growth, $ZrO_2$ plates were used as substrates, and Fig. 4 shows the micrographs of films grown on the bottom face of horizontally held $ZrO_2$ disks. The composition Si/Al=600 results in a continuous ZSM-5 film on the support, but the aluminum-free solution leads only to discrete zeolite particles on the surface. Thus aluminate appears essential for the formation of a continuous zeolite film under the strongly alkaline conditions used in this work, consistent with the observation that aluminate promotes gelation.[43] However, silicalite films can be grown in the complete absence of aluminum at lower alkalinity where the solubility of silica is lower.[23-27] The role of aluminum in gelation had been identified in earlier work of Iler who documented that a trace amount of aluminate can substantially reduce the solubility of silica,[44] and of Harvey and Glasser who reported that aluminum acts as a cross-linking agent in the condensation of aluminosilicates.[45]

The sodium content of the films listed in Table 1 is also of some interest. With the exception of the film grown from a solution with Si/Al=300, the films have similar

sodium contents, about 2 $Na^+$ per 96 T (Si or Al) atoms, or, per unit cell if the solid has fully crystallized. The incorporation of $Na^+$ into zeolites probably occurs at defect sites. Depending primarily on the alkalinity of the reaction mixture the uptake has generally been from 0 to 4 $Na^+$ per unit cell in ZSM-5,[39,46,47] although an extreme case of 7.7 $Na^+$/u.c. was also reported.[41] The high $Na^+$ content in the case of Si/Al=300 suggests that this gel has a different composition, possibly caused by faster gelation at the higher aluminate concentration. It is not immediately obvious, however, whether the elevated sodium uptake inhibits zeolitization. $Na^+$ was reported to impede nucleation and crystallization of silicalite in aluminum-free mixtures.[46,48] But for reaction mixtures containing aluminate, sodium ions actually facilitate crystallization,[32,37] probably by acting as more effective charge compensators than the bulky $TPA^+$ during the incorporation of framework aluminum.[49] Moreover, the effect of sodium was also found to depend on the amount of sodium and silica source used in the synthesis.[26]

***Other effects of the support***

In the previous section alumina supports were shown to influence the crystallinity and elemental composition of the film and powder precipitates by releasing aluminate ions in the strongly alkaline synthesis solution. In this section different functions of alumina and some other surfaces in film formation are examined.

Surprisingly, for certain solution compositions, alumina supports accelerated zeolitization in the bulk of the solution. In the absence of a support, 150 ml solution of Si/Al=600 in 16 h reaction produced less than 0.1 g of amorphous precipitate and only

after 90 h had the precipitate became ZSM-5. By contrast, in the presence of a nonporous alumina disk, under otherwise identical conditions, 0.4 g of ZSM-5 powder was produced in 16 h. A zirconia support under the same conditions also induced a fully crystalline precipitate within 16 h. One possibile explanation of this acceleration of crystallization in the bulk by alumina and zirconia supports is as follows. Small colloidal particles are attracted to the solid surface by dispersion forces and agglomerate there to larger aggregates that provide the preferential sites of nucleation and crystallization. These aggregates assemble into the observed surface gel layer, but some aggregates may become detached to the bulk solution where they are converted to crystalline particles. The function of the support in this scheme is to accelerate primary particle aggregation so that the resulting particles have relatively low aluminate content. Nucleation according to this hypothesis is associated with aggregated particles and not with the primary particles. Aggregation also takes place in the bulk facilitated by aluminate ions but the resulting aggregates are slower to nucleate because of their higher aluminum content. We are led then to distinguish between particles aggregated in the bulk that are slow to nucleate and particles aggregated at the surface easier to nucleate.

To further elucidate the possible distinction between the active and inactive aggregated particles, the effect of placement of the supports in the solution was studied. A non-porous alumina disk was laid horizontally at the bottom of a solution having Si/Al=600. As shown in Fig. 5, 16 h reaction at 175°C results in a gel layer on the top surface of the disk, but the bottom surface contains only discrete zeolite particles. Similar results were observed when using a $ZrO_2$ plate. In contrast, when the supports were

placed just below the top of the solution, the surface gel layers turned completely crystalline after 16 h reaction. These differences suggest that the top face of the plate placed at the bottom of the autoclave is inundated by the relatively inactive particles settling down by gravity while the bottom face does not receives settling particles and develops only discrete zeolite particles. A continuous film fails to develop at the bottom face because of restricted access to nutrients. If the substrate is placed near the top of the solution the gel layer forms primarily by attraction and aggregation of small primary particles moving by Brownian motion while the larger, less active particles are more likely to settle down by gravity. Additional support for the distinction between the two types of particles is furnished by the EDS results listed in Table 2, which show that the gel deposited at the top surface of disks placed at the bottom of the autoclave has composition similar to that of the precipitates formed in the absence of supports. Both have relatively large aluminum and sodium contents.

It has been previously reported that zeolitization is initiated on colloidal particles, even in cases of nominally homogeneous nucleation from a clear solution. Jansen et al. found that an aluminum-free clear solution failed to crystallize, and that traces of ions such as aluminate were necessary for the formation of gel particles that were subsequently transformed into zeolite crystallites.[43] Cundy et al. suggested that homogeneous nucleation is actually associated with amorphous gel or colloidal material in the clear solution.[50] At high alkalinity, zeolitization in a clear solution was found to proceed in the complete absence of gelation, but at a very low rate.[37,42] Based on SAXS-WAXS experiments, Beelen et al. concluded that silicalite nucleation in a clear solution

can proceed via a gel organization mechanism.[51] Primary particles of radius smaller than 1.6 nm aggregate to larger gel particles which become the sites of nucleation. This particular observation offers some support for the previously suggested premise that some degree of aggregation is necessary before nucleation can take place. Direct HREM observation of the emergence of nuclei inside gel nanoparticles was made by Tsapatsis et al.[52] and Mintova et al.[53]

For comparison purposes experiments were also carried out using quartz disks but in contrast with alumina and zirconia, no gel layer was formed on the bottom surface of the disk after 16 h in a reaction mixture of Si/Al=600. During the 16 h period amorphous powder precipitates accumulated at the bottom of the autoclave. When aluminum-free solution was used, zeolite powders precipitated at the bottom of the autoclave after 16 h reaction, but again there was no film at the bottom face of the substrate. The inability of quartz to initiate surface gelation, in contrast with alumina and zirconia, can be explained in terms of the dispersion force between supports and gel particles. Under alkaline hydrothermal conditions, the surface hydroxyl groups of aluminosilicates are completely ionized and negatively charged. These charges are shielded by $Na^+$ and $TPA^+$ cations in the electric double layers. Interactions beyond the Debye length are thus dominated by dispersion forces.[54] Silica is known to be unique among oxides in that its sol is stable at the point of zero charge (pzc), seemingly in contradiction with DLVO theory.[44] This abnormality can be attributed to the weak dispersion force of silica particles.[55] Quantitatively, the dispersion interaction can be characterized by the non-zero frequency

Hamaker constant $A_{v>0}$,[56] and the dispersion energy between a surface and a sphere is given by

$$F=-A_{v>0}R/(6D),$$

where $R$ is the radius of the sphere and $D$ the shortest distance between the sphere and the surface. The estimated Hamaker constants between two media across water are listed in Table 3. The silica-silica interaction is the weakest, accounting for the weak particle-surface interaction. This argument can be also be used to explain why the walls of the Teflon-coated autoclaves in contact with the solution used in this work do not initiate zeolite layer formation.

***Characterization of internal deposits by gas adsorption***

The experiments described so far focused on the morphology of zeolite films grown on the solid surface outside of the porous matrix. Aluminosilicate products also accumulate inside the pores and usually account for the major portion of the weight gain on the tube. The nature of these internal deposits is, therefore, of fundamental interest to zeolite membranes.

Ar and *iso*-butane adsorption measurements are shown in Fig. 5. Uptake peaks were observed only after calcination removed the pore-blocking of TPA template molecules. Both isotherms of the calcined tube show the stepped shape characteristic of ZSM-5 or silicalite for these two adsorbates.[57-60] Quantitatively, the step in the Ar isotherm occurring at occupancy of 23 adsorbate molecules per unit cell is associated

with the phase transition of adsorbed Ar from a less ordered phase to an ordered one.[58] *Iso*-butane adsorption shows a step at 4 molecules/u.c. due to the filling of intersections.[60] Assuming that adsorption occurs in zeolitic pores alone allows to calculate the amount of zeolite on the tube as 9.3 and 9.1 mg/g-tube based on Ar and *iso*-butane adsorption respectively. The good agreement of the two values offers evidence that adsorption at pressures below the steps of the isotherm is limited to zeolitic micropores in the product. The pore size of the remaining 60% amorphous part of the reaction product cannot be ascertained from these measurements.

## 2.4 Conclusions

Hydrothermal synthesis of ZSM-5 films under strongly alkaline compositions is mediated by formation of a precursor gel layer on the support. Supports having a high Hammaker constant and the presence of some aluminates are identified as necessary for the formation of the layer under the conditions of this study. Subsequent zeolitization occurs inside the gel layer. Under certain conditions the support also accelerates crystallization in the bulk of the solution.

Aluminate ions added to the synthesis mixture or leached from the substrate are found to have dual roles in the film growth. On the one hand they facilitate the formation of the gel layer on the support, but on the other hand they retard zeolitization in this gel layer. A substantial fraction of the aluminosilicate product formed inside the pores of the substrate remains amorphous, evidently because of the higher level of aluminate there.

## Acknowledgement

This study was funded by NSF grant CTS 9504901 and by Chevron Research and Technology Co.

## References

[1] E. R. Geus, M. J. den Exter and H. van Bekkum, J. Chem. Soc. Faraday Trans. 88 (1992) 3101.

[2] M. D. Jia, B. S. Chen, R. D. Noble and J. L. Falconer, J. Membrane Sci. 90 (1994) 1.

[3] Y. S. Yan, M. E. Davis and G. R. Gavalas, Ind. Eng. Chem. Res. 34 (1995) 1652.

[4] Z. A. E. P. Vroon, K. Keizer, M.J. Gilde, H. Verweij and A.J. Burggraaf, J. Membrane Sci. 113 (1996) 293.

[5] K. Kusakabe, S. Yoneshige, A. Murata and S. Morooka, J. Membrane Sci. 116 (1996) 39.

[6] M.C. Lovallo and M. Tsapatsis, AIChE J. 42 (1996) 3020.

[7] H.H. Funke, A.M. Argo, C.D. Baertsch, J.L. Falconer and R.D. Noble, J. Chem. Soc. Faraday Trans. 92 (1992) 2499.

[8] J. Coronas, J.L. Falconer and R.D. Noble, AIChE J. 43 (1997) 1797.

[9] R. Lai and G. R. Gavalas, Ind. Eng. Chem. Res. 37 (1998) 4275.

[10] K. Aoki, K. Kusakabe and S. Morooka, J. Membrane Sci. 141 (1998) 197.

[11] K. Kusakabe, T. Kuroda, A. Murata and S. Morooka, Ind. Eng. Chem. Res. 36 (1997) 649.

[12] J.H. Dong and Y.S. Lin, Ind. Eng. Chem. Res. 37 (1998) 2404.

[13] L.X. Zhang, M. D. Jia and E. Min, Stud. Surf. Sci. Catal. 105 (1997) 2211.

[14] J.C. Poshusta, V.A. Tuan, J.L. Falconer and R.D. Noble, Ind. Eng. Chem. Res. 37 (1998) 3924.

[15] N. Nishiyama, K. Ueyama and M. Matsukata, AIChE. J. 43 (1997) 2724.

[16] Y.G. Yan, S.R. Chaudhuri and A. Sarkar, Chem. Mater. 8 (1996) 473.

[17] A. Erdem-Senatalar, H. van Bekkum and J. C. Jansen. Stud. Surf. Sci. Catal. 98 (1994) 30.

[18] T. Nakazawa, M. Sadakata and T. Okubo, Microp. Mesop. Mat. 21 (1998) 325.

[19] H.W. Deckman, A.J. Jacobson, J.A. McHenry, K. Keizer, A.J. Burgraaf, Z.A.E.P. Vroon, L.R. Czarnetzki, F.W. Lai, A.J. Bonus, W.J. Mortier, J.P. Verduijn and E.W. Corcoran, International Patent, PCT WO 94/25151 (1994).

[20] W. Lai, W.H. Deckman, J. A. McHenry and J. P. Verduijn, International Patent, PCT WO 96/01687 (1996).

[21] J. Hedlund, B. J. Schoeman and J. Sterte, Stud. Surf. Sci. Catal. 105 (1997) 2203.

[22] A. Gouzinis and M. Tsapatsis, Chem. Mater. 10 (1998) 2497.

[23] J. C. Jansen and G. M. van Rosmalen, J. Crystal Growth 128 (1993) 1150.

[24] J. C. Jansen, W. Nugroho and H. van Bekkum, in R. von Ballmoos, J.B. Higgins, M.M.J. Treacy (Editors), Proceedings of 9th International Zeolite Conference (Montreal, 1992), Butterworth-Heinemann, Boston, 1993, pp. 247.

[25] J.H. Koegler, H.W. Zandbergen, J.L.N. Harteveld, M.S. Nieuwenhuizen, J.C. Jansen and H. van Bekkum, Stud. Surf. Sci. Catal. 84 (1994) 307.

[26] J.H. Koegler, H. van Bekkum and J.C. Jansen, Zeolites 19 (1997) 262.

[27] M. J. den Exter, H. van Bekkum, C. J. M. Rijn, F. Kapteijn, J. A. Moulijn, H. Schellevis and C. I. N. Beenakker, Zeolite 19 (1997) 13.

[28] V. Valtchev, S. Mintova, B. Schoeman, L. Spasov and L. Konstantinov, Stud. Surf. Sci. Catal. 97 (1995) 527.

[29] J.H. Dong, K. Wegner and Y.S. Lin, J. Membrane Sci. 148 (1998) 233.

[30] Z.A.E.P. Vroon, Ph.D. Dissertation, Twente University, Netherlands, 1995.

[31] W. Kern and D. A. Puotinen, RCA Reviews 31 (1970) 187.

[32] L.D. Rollmann and E.W. Valyocsik, European Patent 0021675 (1983).

[33] H. Nakamoto and H. Takahashi. Chem. Lett. (1981) 1739.

[34] G. Giannetto, F. D. Santos, R. Monque, R. Galiasso and Z. Gabelica, Zeolites 15 (1995) 719.

[35] R. Szostak, Molecular sieves: principles of synthesis and identification, Van Nostrand Reinhold, New York, 1989.

[36] G. Golemme, A. Nastro, J.B. Nagy, B. Subotic, F. Crea and R. Aiello, Zeolites 11 (1991) 776.

[37] A.E. Persson, B.J. Schoeman, J. Sterte and J.-E. Otterstedt, Zeolites 15 (1995) 611.

[38] A. Iwasaki, T. Sano and Y. Kiyozumi, Microp. Mesop. Mat. 25 (1998) 119.

[39] E.G. Derouane, S. Detremmerie, Z. Gabelica and N. Blom, Appl. Catal. 1 (1981) 201.

[40] T. Sano, Y. Kiyozumi, K. Maeda, M. Toba, S. Niwa and F. Mizukami, in R. von Ballmoos, J.B. Higgins, M.M.J. Treacy (Editors), Proceedings of 9th International Zeolite Conference (Montreal, 1992). Butterworth-Heinemann, Boston, 1993, pp. 239.

[41] F. Testa, R. Szostak, R. Chiappetta, R. Aiello, A. Fonseca and J.B. Nagy, Zeolites 18 (1997) 106.

[42] B.J. Schoeman, J. Sterte and J.-E. Otterstedt, Zeolites 14 (1994) 568.

[43] J. C. Jansen, C.W.R. Engelen and H. van Bekkum, in M.L. Occelli and H.E. Robson(Editors), Zeolite Synthesis (ACS Symposium Ser. 398), Washingtong, D.C., 1989, pp. 257.

[44] R.K. Iler, The Chemistry of Silica, Wiley, New York (1979).

[45] G. Harvey and D.L.S. Glasser, in M.L. Occelli and H.E. Robson (Editors), Zeolite Synthesis (ACS Symposium Ser. 398), Washingtong, D.C., 1989, pp. 49.

[46] D.T. Hayhurst, A. Nastro, R. Aiello, F. Crea and G. Giordano, Zeolites 8 (1988) 416.

[47] S.G. Fegan and B.M. Lowe, J. Chem. Soc., Faraday Trans. 1, 82 (1986) 785.

[48] K.J. Chao, T.C. Tasi, M.S. Chen and I. Wang, J. Chem. Soc., Faraday Trans. 1, 77 (1981) 547.

[49] R. de Ruiter, J.C. Jansen and H. van Bekkum, Zeolites 12 (1992)56.

[50] C.S. Cundy, B.M. Lowe and D.M. Sinclair, J. Crystal Growth 100 (1990) 189.

[51] T.P.M. Beelen, W.H. Dokter, H.F. van Garderen and R.A. van Santen, in M.L. Occelli and H. Kessler (Editors), Synthesis of Porous Materials, Zeolites, Clays, and NanosTructures, Marcel Dekker, New York, 1997, pp. 59.

[52] M. Tsapatsis, M. Lovallo and M.E. Davis, Microp. Mat. 5 (1996) 381.

[53] S. Mintova, N.H. Olson, V. Valtchev and T. Bein, Science 283 (1999) 958.

[54] R.J. Hunter, Zeta Potential in Colloidal Science: Principles and Applications, Academic Press, London, 1981.

[55] F. Dumont, in H.E. Gergna (Editor), The Colloidal Chemistry of Silica, ACS, Washington, 1994, pp. 143.

[56] J.N. Israelachivili, Intermolecular and Surface Forces, 2nd ed., Academic Press, San Diego, 1992.

[5757] U. Muller, K.K. Unger, D. Pan, A. Mersmann, Y. Grillet, F. Rouquerol and J. Rouquerol, Stud. Surf. Sci. Catal. 46 (1989) 625.

[58] P.L. Lewellyn, J.P. Coulomb, Y. Grillet, J. Patarin, H. Lauter, H. Reichert and J. Rouquerol, Langmuir 9 (1993) 1846.

[59] S.W. Webb and W.C. Conner, Stud. Surf. Sci. Catal. 62 (1990) 31.

[60] T.J.H. Vlugt, W. Zhu, F. Kapteijn, J. A. Moulijn, B. Smith and R. Krishna, J. Am. Chem. Soc. 120 (1998) 5599.

**Table 2-1** Aluminum and sodium contents of membranes prepared on porous alumina tubes using $6SiO_2$- TPAOH- 4NaOH- $xAl_2O_3$- $571H_2O$ after 16 h reaction at 175°C.

| Support | Solution Si/Al | Film | |
|---|---|---|---|
| | | Si/Al | Na/96T[a)] |
| $Al_2O_3$ | 300 | 13±3 | 8.7±1.5 |
| $Al_2O_3$ | 600 | 21±1 | 1.9±0.5 |
| $Al_2O_3$ | 1200 | 105±25 | 2.0±0.4 |
| $Al_2O_3$ | ∞ | 225±144 | 1.5±0.4 |

a) T atoms: Al or Si. One unit cell of MFI zeolite has 96 T atoms.

**Table 2-2** Aluminum and sodium contents of films prepared on $ZrO_2$ substrates by $6SiO_2$- TPAOH- 4NaOH- 0.01Al- $571H_2O$ after 16 h reaction at 175°C.

| Support Position | Face | Product | |
|---|---|---|---|
| | | Si/Al | Na/96T[a)] |
| No support | Powder | 10±1 | 4.1±1.9 |
| @top | Bottom | 188±78 | 2.0±0.5 |
| @bottom | Top | 5.3±2.5 | 4.9±1.5 |
| @bottom | Bottom | 358±152 | 1.2±0.5 |

a) T atoms: Al or Si. One unit cell of MFI zeolite has 96 T atoms.

**Table 2-3** Hamaker constants $A_{v>0}$ ($10^{-20}$) for two media interacting across water[a].

| | $SiO_2$ | $Al_2O_3$ | $ZrO_2$ |
|---|---|---|---|
| $SiO_2$ | 0.35 | 1.2 | 2.1 |
| $Al_2O_3$ | 1.2 | 4.1 | 7.3 |

a) estimated from the expression and constants in Ref. 56.

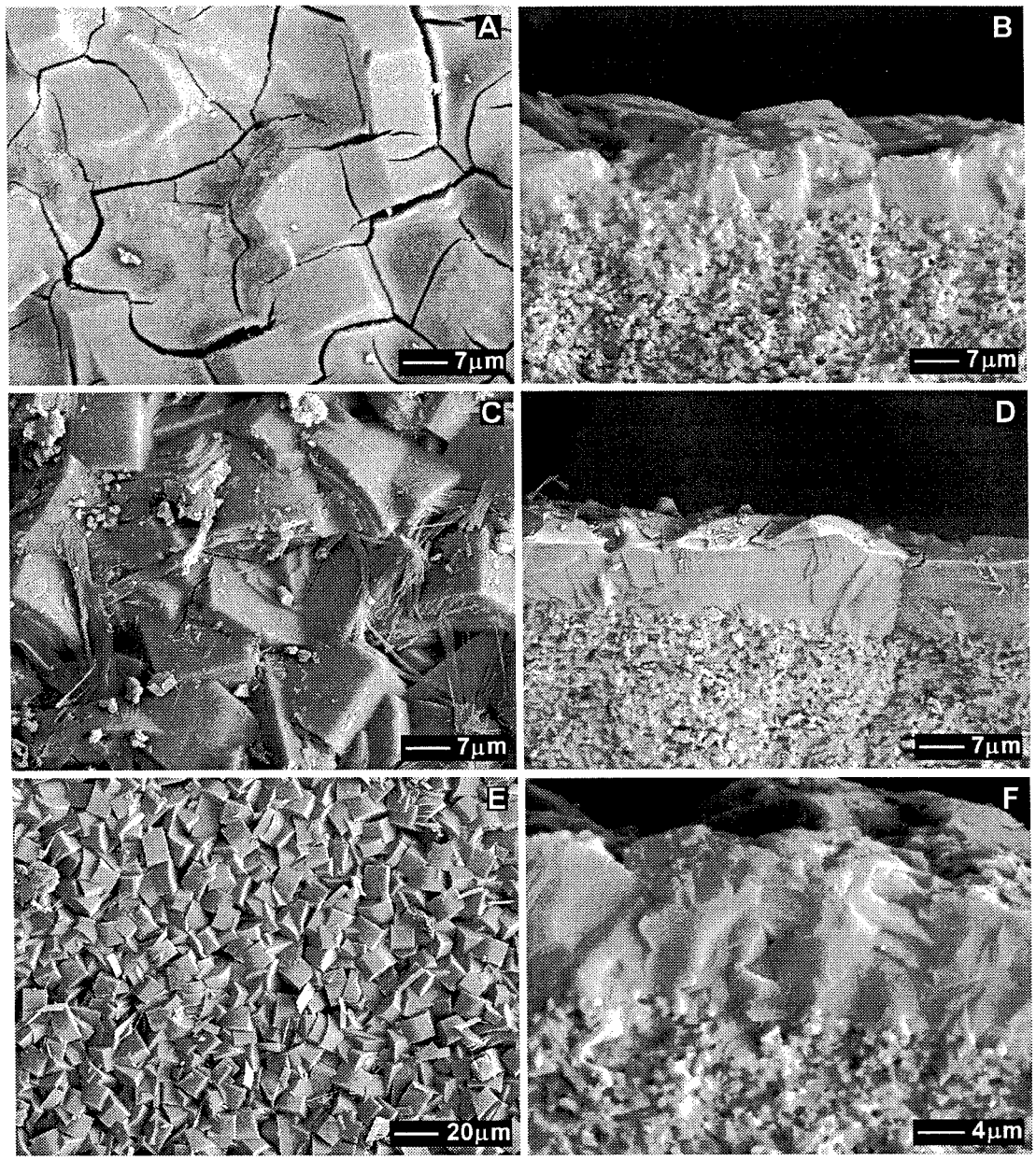


**Figure 2-1** SEM micrographs of the zeolite film growing on porous $\alpha$-$Al_2O_3$ tubes at 175°C in the solution $6SiO_2$: TPAOH: 4NaOH: $571H_2O$ after: (A,B) 8 h; (C,D) 12 h; (E,F) 16 h. B, D, F are cross sections.

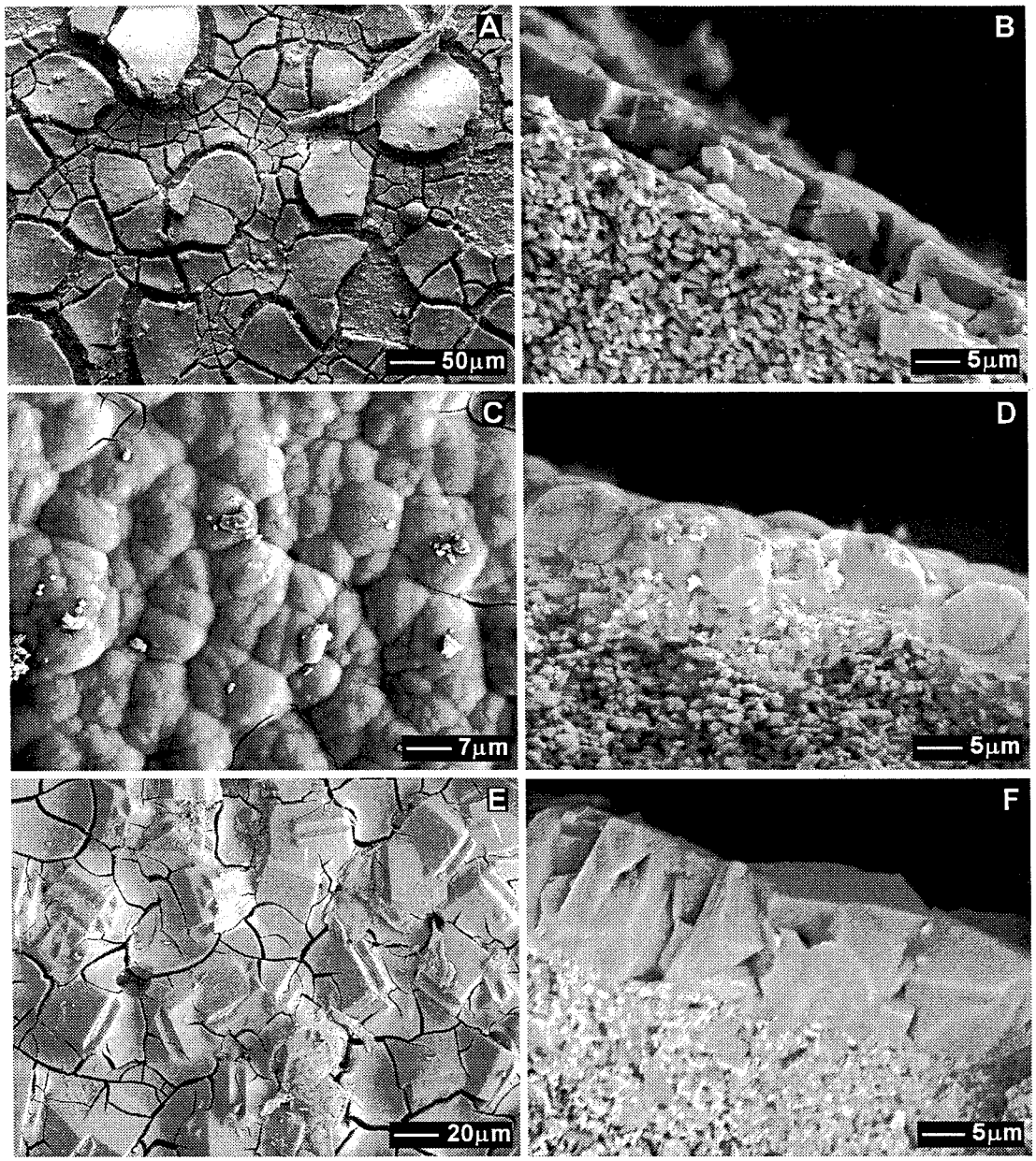


**Figure 2-2** SEM micrographs of films growing on porous $\alpha$-$Al_2O_3$ tubes after 16 h reaction at 175°C in a solution with Si/Al=300 (A,B); 600 (C,D); 1200 (E,F), where B, D, F are side views. The film grown in an Al-free solution is shown in Fig. 1E,F.

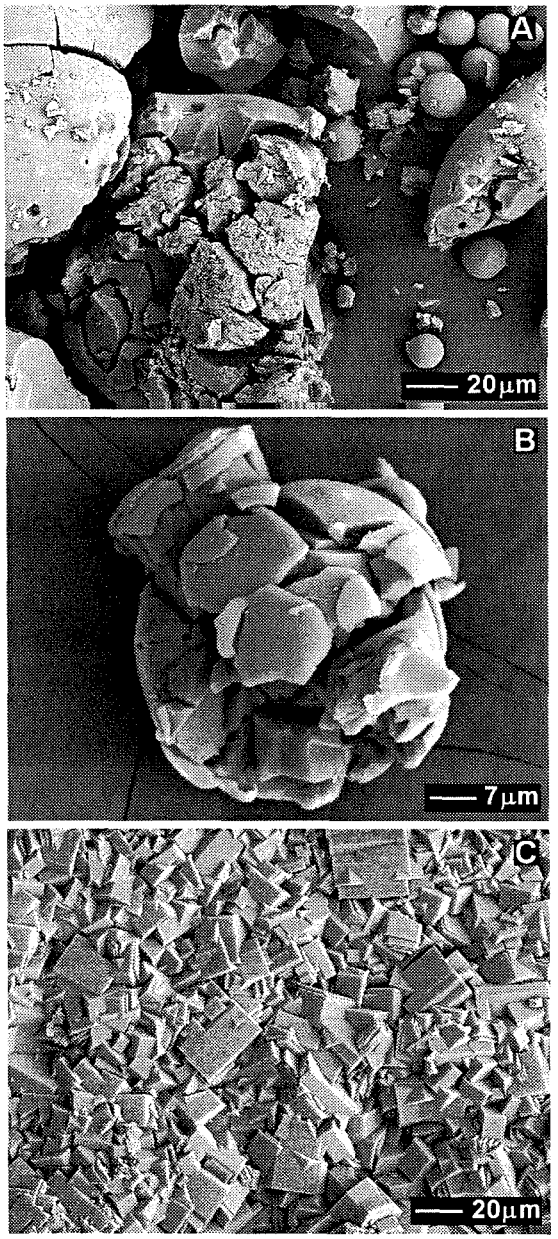


**Figure 2-3** SEM micrographs of precipitates formed in a solution with $6SiO_2$: TPAOH: 4NaOH: 0.01Al: $571H_2O$ in the absence of a support after reaction at 175°C for different times: (A) 16 h; (B) 48 h; (C) 90 h.

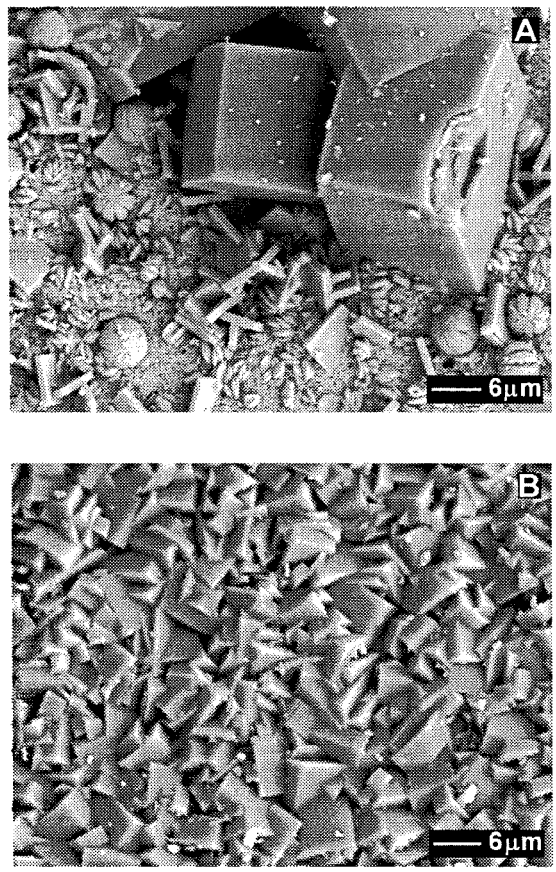


**Figure 2-4** SEM of the bottom face of a $ZrO_2$ plate held just below the surface of a solution with $6SiO_2$: TPAOH: 4NaOH: $x$Al: $571H_2O$ at 175°C for 16 h. (A) $x$=0; (B) $x$=0.01.

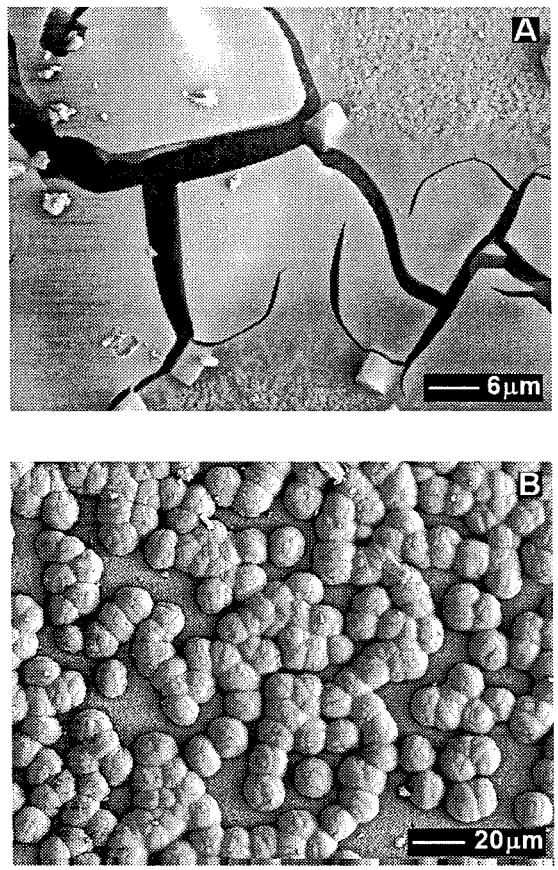


**Figure 2-5** SEM micrographs of the surfaces of an alumina plate held for 16 h at 175°C at the bottom of the autoclave in a solution with $6SiO_2$: TPAOH: 4NaOH: 0.01Al: $571H_2O$. (A) top surface of the plate; (B) bottom surface.

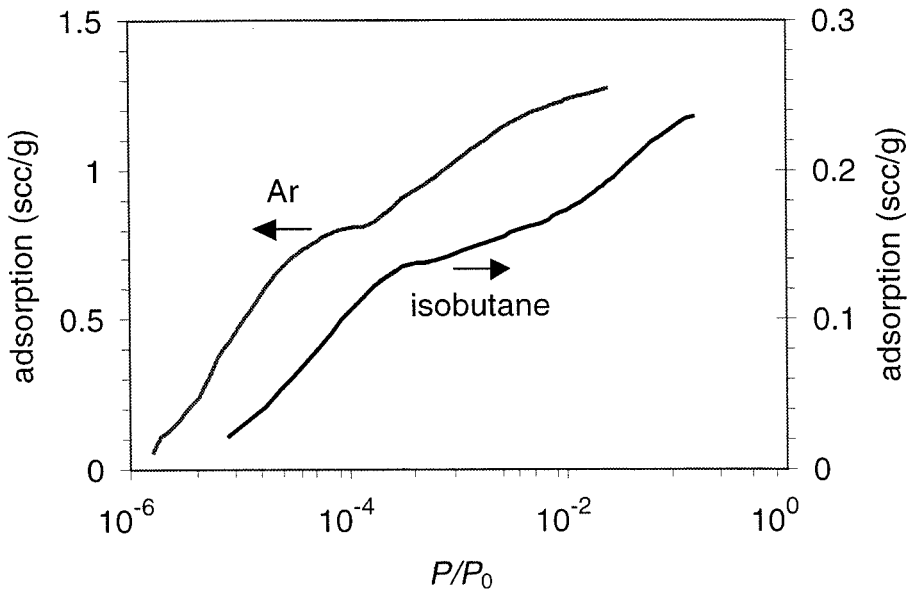


**Figure 2-6** Ar (77 K) and *iso*-butane (273 K) adsorption isotherms of a zeolite membrane grown on a porous tube based on the differences of adsorption between the calcined and uncalcined tube. The steps in the isotherms correspond to 23 (Ar) and 4 (iso-butane) molecules per unit cell.

**Chapter 3**

# Surface Seeding in ZSM-5 Membrane Preparation

Reproduced with permission from *Ind. Eng. Chem. Res.* **1998**, *37*, 4275-4283

# Surface Seeding in ZSM-5 Membrane Preparation

Re Lai and George R. Gavalas

*Division of Chemistry and Chemical Engineering, California Institute of Technology*

*Pasadena, California 91125*

## Abstract

ZSM-5 zeolite membranes were prepared by *in situ* hydrothermal synthesis on macroporous α-alumina tubes coated with silicalite seeds. Seed particles were prepared by hydrothermal synthesis at 95°C to mean size 0.4 or 2 μm, purified of unconverted reactants and suspended in a buffered aqueous solution. The support tubes were seeded by immersion in the particle suspension under ultrasonication. Membrane growth on seeded supports was carried out at temperatures 110-150°C and different reaction times. SEM of the membrane top surface and cross section of the supports indicates gradual growth of an external polycrystalline layer and accumulation of siliceous deposits as deep as 100 μm inside the pores of the support. Thermogravimetric analysis and nitrogen and argon adsorption measurements indicate graduate conversion of deposits from amorphous to crystalline. Pure gas permeation results are presented for membranes prepared using 0.4 and 2 μm seeds under different compositions and temperatures.

## 3.1 Introduction

Zeolite membrane synthesis has drawn increasing attention in recent years on account of new opportunities for separations of gases and liquid mixtures. In contrast to amorphous carbon or silica molecular sieving membranes, zeolites offer well-defined crystalline structures with uniform and tuneable micropores. Zeolite membranes also compare favorably with polymeric membranes in terms of durability, mechanical strength, chemical resistance, and separation selectivity.

The last five years have witnessed significant progress in zeolite membrane synthesis.[1,2] Preparation is generally carried out by growing a continuous layer on a porous support under hydrothermal reaction conditions. Such continuous zeolite layers must develop from surface nuclei growing into interlocking crystallites and thus eliminating interzeolitic pathways. Most of zeolite membranes prepared so far involve the MFI-type zeolite ZSM-5 and its aluminum-free analogue silicalite.[2-8] ZSM-5 membranes have shown impressive separation properties for hydrocarbon gas mixtures and for water-organic mixtures.[2] For example, selectivities or separation ratios of 50-100 have been demonstrated for *n*-butane : isobutane[8] and *n*-heptane : isooctane.[9] Other types of zeolite membranes such as A-type[10] and AFI[11] have also been reported.

While heterogeneous nucleation and crystallite intergrowth are recognized as necessary for the formation of a continuous zeolite film, the mechanism by which they proceed is not well understood. Investigations suggest that membrane growth often starts with formation of a gel layer on the support surface.[12,13] Crystallites subsequently

develop out of this gel to form an intergrown layer. It has been observed that the structure of the crystalline layer is sensitive to the synthesis mixture composition,[6,14] the composition of the support[3] and the position of the support in the synthesis autoclave[13]. All these factors interact in a complicated manner, resulting in a narrow window of conditions for growth of good quality membranes. Identification of these favorable conditions requires extensive trial and error, and understanding of the effect of individual variables remains elusive.

The range of conditions for successful membrane growth may be expanded by using seeding, a technique that has been extensively used in bulk zeolite synthesis. Its application to membrane preparation involves attaching a closely packed layer of zeolite particles on the substrate surface, which in subsequent hydrothermal reaction grow to fill the interparticle voids. The need for heterogeneous nucleation is thereby eliminated and the window of conditions for development of a continuous film is expanded. Seeding has been used previously by several groups in zeolite membrane preparations. Deckman et al. coated porous tubes with a slurry containing silica gel and ZSM-5 seeds to grow ZSM-5 membranes.[15] Tsapatsis and collaborators carried out a series of studies on the preparation of unsupported and supported films by secondary growth of zeolite particle layers. Thus, Lovallo and Tsapatsis prepared unsupported and supported films of zeolite L by regrowing particle layers deposited from a mixed suspension of zeolite L particles (~60 nm) and boehmite particles.[16] Lovallo and Tsapatsis prepared unsupported and supported layers from suspensions of silicalite particles (~100 nm) and boehmite particles.[17] The supported layers were deposited by repeated dip-coating and drying on

glass slides or silicon wafers. Regrowth of both unsupported and supported particle layers resulted in continuous films of submicron thickness. Zeolite A particle layers were also prepared by repeated dip coating of nonporous supports in a suspension of colloidal zeolite A particles (200~300 nm) followed by regrowth to a continuous film of submicron thickness.[18] Porous alumina tubes were seeded by simple rubbing with Na-X zeolite particles to yield after hydrothermal synthesis Y-type zeolite membranes with useful permselectivities between $N_2$ and $CO_2$.[14] Surface seeding was also used to prepare ultra-thin silicalite and zeolite A type films (80~800 nm) on gold and silicon wafer surfaces.[19-21]

In this paper we report a simple technique for coating porous $\alpha$-$Al_2O_3$ tubes with silicalite particles and examine membrane growth on the seeded surfaces focusing on the effects of seed particle size and reaction conditions on membrane morphology and permeation properties.

## 3.2 Experimental

### *Materials*

Tetrapropylammonium hydroxide (TPAOH, 1.0 M solution, Aldrich) and NaOH (99.99%, Aldrich) were used as provided. Tetraproylammonium bromide (TPABr, 98%, Aldrich) was dissolved in water and filtered with 0.22 μm cellulose acetate membranes (VWR). The silica source was tetraethylorthosilicate (TEOS, 98%, Aldrich and Alfa Aesar). Two types of $\alpha$-$Al_2O_3$ substrates were used in this study: thin, non-porous plates

(99.6%, Coors Ceramics) and symmetric porous tubes of 6~7 mm ID, 9~10 mm OD, 0.2 μm mean pore diameter, and *ca.* 30% void fraction (Golden Technologies).

***Surface seeding***

Silicalite seed preparation was based on the protocol of Persson et al.[22] Seeds of 0.4 μm mean size were synthesized from a solution of $SiO_2$: 0.2TPAOH: 0.08NaOH: $60H_2O$, kept at 95°C for 50 h. Seeds of 2 μm mean size were prepared from a solution of $SiO_2$: 0.12TPAOH: 0.008NaOH: $60H_2O$, kept at 95°C for one week. The particles were separated by repeated centrifugation and decanting until the supernatant was washed to neutral. Their phase was confirmed by XRD.

A colloidal silicalite suspension was prepared by dispersing the silicalite particles in pH buffers (VWR) at concentration of 0.33 wt % for 0.4 μm seeds and 1.3 wt % for 2 μm seeds. The substrate was immersed in the suspension under ultrasonication for 1 h, then withdrawn and dried in air.

***Hydrothermal growth on seeded supports***

Before hydrothermal reaction, the seeded substrate was heated to 250°C for 1 h to enhance the attachment of the zeolite particles by condensation of their surface hydroxyl groups with those of the support. The substrate was then washed with water to remove the buffer electrolytes and dried at 110°C.

The synthesis solution was prepared by mixing and stirring the reagents NaOH, TPABr, water and TEOS at room temperature for one day. The support tube was placed horizontally or vertically using a Teflon holder in a 250 ml Teflon-lined stainless steel autoclave. A closely fit Teflon rod was inserted in the bore of the tube so that the membrane could only grow at the outer surface. After fixing the tube and adding 150 ml solution, the autoclave was placed in a forced convection oven preheated at the desired temperature. After completion of the specified reaction time the autoclave was removed, cooled and opened and the membrane was thoroughly washed and dried in air. Although the synthesis solution was prepared without aluminum, leaching of the support in the highly alkaline solution introduces a certain amount of aluminum in the solution and in the zeolite layer growing around the silicalite seeds. In recognition of this intrusion of aluminum, the resulting membrane is denoted as ZSM-5 rather than silicalite although its elemental composition was not examined.

***Characterization***

SEM (Camscan, 15 kV) was used to examine the morphology of the zeolite films. The crystalline phase of the film was confirmed by XRD. Nitrogen and argon adsorption of uncalcined and calcined membranes was carried out by the static volumetric method at 77 K using an ASAP 2000 instrument. Before adsorption, the uncalcined tubes were degassed at 180°C overnight, and the calcined tubes were degassed at 350°C overnight. TGA measurements were conducted with 1 g sample and a heating rate of 3 K/min.

To conduct permeation measurements the membranes were calcined to 450-500°C under vacuum at a heating rate of 1°C/min and kept at the final temperature under oxygen flow for at least additional 10 h. Such a scheme may be useful in preventing cracks.[23] After calcination, the tubes were mounted on Pyrex tubing using an epoxy resin (Varian). Permeation measurements were conducted by the pressure rise technique following the procedure described by Yan et al.[6] The outer side of the tube was fed with a pure gas at atmospheric pressure, and the inner side was evacuated. When the vacuum side was shut off from the vacuum pump, its pressure rise was recorded by a pressure transducer and converted to the gas flux across the membrane.

## 3.3 Results and discussion

### *Surface seeding*

A major variable affecting the coverage of the support by seeds was the pH of the seed suspension. The points of zero charge (pzc) of alumina and silicalite are pH=9 and pH=7, respectively.[24,25] Therefore, setting the pH between these two values results in a negatively charged silicalite surface and a positive charged alumina surface, maintaining a favorable electrostatic interaction between the two oppositely charged surfaces.

Experimental results confirm the role of suspension pH. Fig. 1 shows the variation of the surface density of 0.4 μm seeds with pH. The best coverage was achieved at pH=8, which is between the pzc's of alumina and silicalite. Outside this pH region the surface density of seeds decreased, indicating an important effect of surface

charging on the seeding process. Figure 2 shows the seeding of porous alumina tubes by 0.4 μm and 2 μm particles. At pH=8 the coverage is good for both particle sizes but pH=5 results in less dense coverage. It is also observed that the larger particles provide a uniform coverage whereas the smaller particles leave bare patches centered around large particles belonging to the surface of the support. Particle coating of porous supports is facilitated by capillary suction as well as electrostatic and dispersion forces which may explain the different coverage attained with the two particle sizes.

Several previous studies of surface coating by zeolite particles were noted earlier. Repeated dip-coating in a suspension was used to obtain essentially monolayers of silicalite and zeolite L particles at neutral pH and and zeolite A ( ZK-4) particles at pH=10.[16-18] It is noted that electrostatic particle-surface interactions are not critical when dip-coating is used for surface seeding. For all three zeolites the particles were highly oriented, e.g., the silicalite particles were oriented with their *c*-axis perpendicular to the film surface and this orientation persisted in subsequent hydrothermal reaction (regrowth). Neutral or negatively charged surfaces can be coated with negatively charged particles by first absorbing a cationic polymer to impart positive charge.[19-21] Yan and Bein utilized bifunctional coupling layers that bind to the gold substrate as well as to the zeolite crystals to attach a zeolite film.[26]

***Effects of surface seeding on membrane synthesis***

The immediate benefit of using seeding is that a high number of nuclei anchored at the surface are ensured. This is vividly demonstrated in Fig. 3. The composition

$10SiO_2$ :TPABr: NaOH: $980H_2O$

by Cundy et al. was used to grow a film at 95°C.[27] As the figure shows, there is only marginal coverage by zeolite crystallites on the unseeded tube, while the zeolitic film on the seeded tube is almost continuous. The interzeolitic voids evident in Fig. 3A suggest that the conditions of this particular synthesis are not good enough for membrane preparation. Lovallo and Tsapasis,[17] and Kusakabe et al.[8] observed similar sparse coverage on an unseeded substrate using reaction conditions which gave a continuous film on a seeded substrate.

Another benefit of surface seeding is the acceleration of zeolitization, as the presence of zeolitic seeds eliminates the induction period. This is shown in an experiment using the solution

$6SiO_2$: TPAOH: 4NaOH: $571H_2O$

at 150°C for 16 h (Fig. 4). This composition was found by Yan et al. to result in strong surface gelation at the beginning of the reaction.[6] As shown in Figure 4, crystallization resulted in an almost continuous film on the seeded surface, while the unseeded tube was still covered with a thick gel layer. The increase of reaction rates in the presence of seeding will be beneficial when shorter reaction times or lower reaction temperatures are desirable.

***Membrane preparation on seeded supports***

Among the synthesis variables, initial $OH^-$ concentration and temperature seem to be the most important with respect to membrane morphology. Figure 5 shows membranes prepared with different $Na_2O$ contents. At low values of $Na_2O$ the SEM plane view shows patches of large crystals or crystal aggregates probably grown in the solution and subsequently attached on the surface layer of smaller crystals deriving from the seeds. At higher $Na_2O$ concentrations homogeneous nucleation appears to be supressed and the membrane layer is much more uniform and well intergrown. As a result the composition

$$20SiO_2: 3TPABr: 7Na_2O : 1953H_2O$$

was selected for membrane preparations. SEM micrographs of ZSM-5 membranes prepared using 0.4 μm and 2 μm seeds after hydrothermal synthesis at 150°C are presented in Fig. 6. Both membranes are continuous with good intergrowth but the membrane prepared using the 2 μm seeds is thicker and contains larger crystals and fewer crystal interfaces. Figure 7 shows membranes synthesized at 130°C and 110°C on supports seeded with 0.4 μm particles. The thickness of the external layers, estimated from cross-section SEM micrographs, are 5, 4 and 2 μm for the membranes prepared at 150, 130 and 110°C, respectively.

***Evolution of membrane properties with time***

To examine the course of zeolitization, a number of membranes were prepared using reaction times of 2, 4, 7 and 16 h, all at 150°C. SEM micrographs of the resulting

membranes are shown in Fig. 8. After 2 h the seeded surface was covered by a thin gel layer but with the progress of time seeds grow and consume the gel, eventually forming a continuous polycrystalline layer. During the same period the membrane thickness increases from 3 μm at 4 h to 10 μm at 16 h.

As previously documented by electron probe microanalysis (EPMA)[28] and by weight gain measurements,[2] hydrothermal synthesis on macroporous supports results in extensive deposition of siliceous materials inside the pores of the support in addition to forming the external crystalline layer. Coronas et al. concluded that the separation properties of some of their membranes are due to crystallites grown inside the pores.[2] Generally, however, the degree of crystallinity and the contribution of the internal layers to the membrane permeance and selectivity have not been examined. An effort was made in the present study to estimate the amount and crystallinity of the internal layer using TGA, $N_2$ and Ar adsorption and mass gain measurements. A TGA trace of a membrane prepared using seeding is presented in Fig. 9. A distinctive peak of TPA template decomposition is observed at *ca.* 350°C, in good agreement with similar patterns observed for silicalite powders[29] and supported MFI membranes.[8]

High resolution gas adsorption, sometimes called HRADS, was conducted for $N_2$ and Ar adsorbates. With high resolution isotherms covering a wide range of pressures ($10^{-6}<P/P_0<1$), this technique is very useful in studying microporous materials.[30] Fig. 10 shows nitrogen adsorption isotherms of uncalcined and calcined membranes. No nitrogen adsorption is observed at $P/P_0<10^{-5}$ for the uncalcined sample, evidently because the TPA molecules block the micropores. After calcination, a take-up peak

corresponding to zeolitic micropores appears at *ca.* $P/P_0 = 10^{-6}$ consistent with the previous results for MFI-type zeolites.[31,32] The substep in the nitrogen isotherm at $P/P_0$~0.2 characteristic of silicalite and high-silica ZSM-5 is not observed here, indicating some aluminum content in the crystalline deposit. A more direct evidence of ZSM-5 growth on the tube is found in the Ar adsorption isotherm (Fig. 11), which contains a distinctive substep corresponding to the transition of the adsorbate into a more ordered phase.[31] The reason why the substep can be observed in the Ar isotherm but not in the $N_2$ isotherm is that lack of quadrapole moment makes Ar far less sensitive to the aluminum content in the adsorbents.

The adsorption, TGA, and mass gain results for the membranes prepared using different reaction times are summarized in Table 1. The thickness of the siliceous layer formed within the porous support is estimated by assuming that the layer is compact and of the same density as silicalite. As can be seen from the table, the thickness of the interior layer gradually increases with time and reaches 100 μm, consistent with previous direct EPMA for flat $\alpha$-$Al_2O_3$ supports of 0.5 μm pore size.[28]

The crystallinity of the deposits can be estimated from either the adsorption or the TGA results. Two approaches were followed to intepret the adsorption results. In the first approach, is was assumed that the difference between adsorption by the calcined and uncalcined tubes is due to zeolitic micropores alone. $N_2$ and Ar isotherms result in essentially the same estimates. In the second approach crystallinity was estimated using the height of the substep in the Ar isotherms corresponding to adsorption from 23 molecules to 30 molecules per unit cell.[31] An advantage of the second approach is that it

ensures the exclusion of the contribution from non-zeolitic micropores. It turns out that the crystallinities estimated in this manner are very close to those obtained from the first approach, suggesting that there is no contribution from non-zeolitic micropores.

To obtain estimates from the TGA traces, it was assumed that all the weight loss above *ca.* 350°C is due to the decomposition of zeolitic TPA, and that the TPA content in the zeolite is the same as that in pure silicalite, $TPA_2O$-$48SiO_2$-$H_2O$.[31] Both are rough approximations, for the weight loss also includes the contribution of non-zeolitic TPA decomposition and continuing loss of $H_2O$. Compared to the adsoption results, TGA analysis tends to overestimate the crystallinity.

***Single gas permeation***

Single gas permeation was carried out to evaluate the zeolite membranes prepared by surface seeding. The results are summarized in Table 2. The pure gas permeances of membranes prepared using 2 μm seeds at 4, 7 and 16 h of reaction at 150°C are listed in the first several rows of the table. With increasing reaction time the membranes, as expected, show lower permeance and higher selectivities. Unfortunately there is large variability among membranes prepared under nominally identical conditions as can be seen by comparing rows 3-5 of the Table. Generally, however, the membranes prepared using the 2 μm seeds despite being twice as thick have higher permeance than those prepared using the 0.4 μm seeds. One possible explanation is the larger number of intergrown crystal boundaries across the membrane prepared using the smaller seed particles resulting in disrupted microporous lattices and, consequently, increased

diffusion resistance. Higher nitrogen and n-butane permeance was obtained for a membrane prepared without the use of seeds but with a different composition. Unseeded membranes were found earlier to have an external layer of 20-50 μm comprising 10-30 μm crystals. By comparison membranes prepared with 2 μm seeds have thickness about 8 μm comprising crystals 4-6 μm. The higher permeance of the unseeded membranes suggest the possibility that the major resistance to permeation is due to the interfaces between the crystals rather than to diffusion inside the crystals. In view of the variability among membranes prepared under nominally identical conditions, this conclusion is very tentative. As discussed earlier the internal deposits must also be considered. Deposits extend as far as 100 μm inside the pores, and during the time needed to form a well-developed external layer, they gradually densify and become more crystalline. So far the relative contribution of the external and internal layers to the permeation properties has not been ascertained and attempts to reduce the internal layer by diffusion barriers have yielded only modest results.[34]

The last row of Table 2 shows higher $N_2$ and n-butane permeance reported by Kusakabe et al.[8] Much higher nitrogen permeances and high $N_2$:$SF_6$ selectivities were reported by Coronas et al.[2] The difference between membrane properties are due to different supports and synthesis protocols used by the different investigators, but the role of the individual variables is not clear at this time.

## 3.5 Conclusion

Porous $\alpha$-$Al_2O_3$ supports can be coated with a dense layer of silicalite particles by simple immersion in a suspension maintained at pH about 8, intermediate between the isoelectric points (IEP's) of the support and silicalite. Zeolite layers grow on the seeded supports at lower temperatures and shorter times than required when using unseeded supports. Homogeneous nucleation during synthesis can be suppressed by using high pH. The resulting membranes have somewhat lower permeance than membranes prepared without using seeds. With both seeded and unseeded supports, the hydrothermal reaction generates extensive partially amorphous material inside the pores that probably adds significantly to the resistance to permeation.

## Acknowledgement

This study was funded by NSF grant CTS 9504901 and by Chevron Research and Technology Company. Micromeritics Corp. provided a grant for the ASAP 2000 instrument.

## References

(1) Bein, T. Synthesis and Applications of Molecular-Sieve Layers and Membranes. *Chem. Mat.* **1996**, *8*, 1636.

(2) Coronas, J.; Falconer, J. L.; Noble, R. D. Characterization and Permeation Properties of ZSM-5 Tubular Membranes. *AIChE J.* **1997**, *43*, 1797.

(3) Geus, E. R.; den Exter, M. J.; van Bekkum, H. Synthesis and Characterization of Zeolite (MFI) Membranes on Porous Supports. *J. Chem. Soc. Faraday Trans.* **1992**, *88*, 3101.

(4) Geus, E. R.; Bakker, W. J. W.; Moulijn, J. A.; van Bekkum, H. High-temperature Stainless Steel Supported Zeolite (MFI) Membranes: preparation, module construction and permeation experiments. *Microporous Mater.* **1993**, *1*, 131.

(5) Bai, C.; Jia, M.; Falconer, J. L.; Noble, R. D. Preparation and Separation Properties of Silicalite Composite Membranes. Abstract in Third International Conference on Inorganic Membranes, Worchester, Massachusetts, July 10-14, 1994.

(6) Yan, Y. S.; Davis, M. E.; Gavalas, G. R. Preparation of Zeolite ZSM-5 Membranes by in-situ Crystallization on Porous $\alpha$-$Al_2O_3$. *Ind. Eng. Chem. Res.* **1995**, *34*, 1652.

(7) Vroon, Z. A. E. P.; Keizer, K.; Gilde, M. J.; Verweij, H.; Burggraaf, A. J. Transport Properties of Alkanes through Ceramic Thin Zeolite MFI Membranes. *J. Membrane Sci.* **1996**, *113*, 293.

(8) Kusakabe, K.; Yoneshige, S.; Murata, A.; Morooka, S. Morphology and Gas Permeance of ZSM-5-type Zeolite Membrane Formed on a Porous $\alpha$-alumina Support Tube. *J. Membrane Sci.* **1996**, *116*, 39.

(9) Funke, H. H.; Argo, A. M.; Baertsch, C. D.; Falconer, J. L.; Noble, R. D. Separation of Close-Boiling Hydrocarbons with Silicalite Zeolite Membran. *J. Chem. Soc. Faraday Trans.* **1996**, 92, 2499.

(10) Masuda, T.; Hara, H.; Kouno, M.; Kinoshita, H.; Kinoshita, H.; Hashimoto, K. Preparation of an A-type Zeolite Film on the Surface of an Alumina Ceramic Filter. *Micropor. Mat.* **1995**, *3*, 565.

(11) Wu, C. N.; Chao, K. J.; Tsai, T. G.; Chiou, Y. H.; Shih, H. C. Oriented Growth of Molecular Sieves on Inorganic Membranes. *Advanced Mat.* **1996**, *8*, 1008.

(12) Koegler, J.H.; Zandbergen, H. W.; Harteveld, J. L. N.; Nieuwenhuizen, M. S.; Jansen, J. C.; van Bekkum, H. Oriented Coatings of Silicalite-1 for Gas Sensor Applications. *Stud. Surf. Sci. Catal.* **1994**, *84*, 307.

(13) Yan, Y. S. Preparation of Zeolite ZSM-5 Membranes. Ph.D. Dissertation, California Institute of Technology, Pasadena, CA, 1996.

(14) Kusakabe, K.; Kuroda, T.; Murata, A.; Morooka, S. Formation of a Y-Type Zeolite Membrane on a Porous α-Alumina Tube for Gas Separation. *Ind. Eng. Chem. Res.* **1997**, *36*, 649.

(15) Deckman, H. W.; Jacobson, A. J.; McHenry, J. A.; Keizer, K.; Burgraaf, A. J.; Vroon, Z. A. E. P.; Czarnetzki, L. R.; Lai, F. W.; Bonus, A. J.; Mortier, W. J.; Verdulin, J. P.; Corcoran, E. W. Molecular Sieve Layers and Processes for their Manufacture. Patent, International Application Number PCT/EP94/01301.

(16) Lovallo, M. C.; Tsapatsis, M. Preparation of an Asymmetric Zeolite L Film. *Chem. Mater.* **1996**, *8*, 1579.

(17) Lovallo, M. C.; Tsapatsis, M. Preferentially Oriented Submicron Silicalite Membranes. *AIChE J.* **1996**, *42*, 3020.

(18) Boudreau, L. C.; Tsapatsis, M. A. Highly Oriented Thin-Film of Zeolite-A. *Chem. Mat.* **1997**, *9*, 1705.

(19) Mintova, S.; Valtchev, V.; Engstrom, V.; Schoeman, B. J.; Sterte, J. Growth of Silicalite-1 Films on Gold Substrates. *Micropor. Mat.* **1997**, *11*, 149.

(20) Hedlund, J.; Schoeman, B. J.; Sterte, J. Synthesis of Ultra-thin Films of Molecular-Sieves by the Seed Film Method. *Stud. Surf. Sci. Catal.* **1997**, *105*, 2203.

(21) Sterte, J.; Mintova, S.; Zhang, G.; Schoeman, B. J. Thin Molecular-Sieve Films on Noble-Metal Substrates. *Zeolites*, **1997**, *18*, 387.

(22) Persson, A. E.; Shoeman, B. J.; Otterstedt, J. E. *Zeolites*, **1994**, *14*, 557.

(23) Lewis, J. E.; Gavalas, G. R.; Davis, M. E. Permeation Studies on Oriented Single-Crystal Ferrierite Membranes. *AIChE. J.* **1997**, *43*, 83.

(24) Hunter, R. J. Zeta Potential in Colloidal Science: Principles and Applications. Academic Press, London, 1981.

(25) Vroon, Z. A. E. P. Synthesis and Transport Studies of Thin Ceramic Supported Zeolite (MFI) Membranes. Ph.D. dissertation, Twente University, Netherlands, 1995.

(26) Yan, Y.; Bein, T. Molecular Recognition on Acoustic Wave Devices: Sorption in Chemically Anchored Zeolite Monolayers. *J. Phys. Chem.* **1992**, *96*, 9387.

(27) Cundy, C. S.; Lowe, B. W.; Sinclair, D. M. Direct Measurement of the Crystal-Growth Rate and Nucleation Behavior of Silicalite, a Zeolitic Silica Polymorph. *J. Crystal Growth* **1990**, *100*, 189.

(28) Yan, Y. S.; Tsapatsis, M.; Gavalas, G. R.; Davis, M. E. Zeolite ZSM-5 Membranes Grown on Porous alpha-$Al_2O_3$. *J. Chem. Soc. Chem. Commun.* **1995**, *2*, 227.

(29) Geus, E. R.; van Bekkum, H. Calcination of Large MFI-type Single Crystals. *Zeolites* **1995**, *15*, 333.

(30) Hathaway, P. E.; Davis, M. E. High Resolution quasi-equilibrium Sorption Studies of Molecular Sieves. *Catal. Today* **1990**, *5*, 333.

(31) Muller, U.; Unger, K. K.; Pan, D.; Mersmann, A.; Grillet, Y.; Rouquerol, F.; Rouquerol, J. High Resolution Sorption Studies of Ar and Nitrogen on large Scale Crystals of Aluminophosphate $AlPO_4$-5 and Zeolitic ZSM-5. *Stud. Surf. Sci. Catal.* ***1989, 46***, 625.

(32) Webb, S. W.; Conner, W. C. Sorption of Gases on Microporous Solids: Pore Size Characterization by Gases Adsorption. *Stud. Surf. Sci. Catal.* **1990**, *62*, 31.

(33) Flanigen, E. M.; Bennett, J. M.; Grose, R. W.; Cohen, J. P.; Patton, R. L.; Kirchner, R. M.; Smith, J. V. Silicalite, a New Hydrophobic Crystalline Silica Molecular Sieve. *Nature* **1978**, *271*, 512.

(34) Yan, Y. S.; Davis, M. E.; Gavalas, G. R. Use of Diffusion-Barriers in the Preparation of Supported Zeolite ZSM-5 Membranes. *J. Membrane Sci.* **1997**, *126*, 53.

**Table 3-1** Characterization of MFI growth process on porous tube seeded by 2 μm crystallites using weight gain, TGA and nitrogen and argon adsorption.

| Reaction time (h) | Weight gain (mg/g) | Film Thickness (μm) | | Crystallinity (%) | | | |
|---|---|---|---|---|---|---|---|
| | | Outer | Inner | TGA | $N_2$[a] | Ar[a] | Ar[b] |
| 2 | 5.1 | 2 | 24 | --- | --- | -- | -- |
| 4 | 11 | 3.4 | 56 | 32 | --- | -- | -- |
| 7 | 17 | 4.3 | 89 | 39 | 16 | 18 | 16 |
| 16 | 22 | 10 | 102 | 64 | 53 | 50 | 47 |

a) from $N_2$ or Ar adsorption amount at $P/P_0$=0.1

b) from Ar adsorption isotherm substep

**Table 3-2** Pure gas permeance of various membranes at 110°C.

| Seed size (μm) | reacn temp (°C) | reacn time (h) | Permeance ($10^{-9}$mol/Pa $m^2$ s) | | Selectivity | |
|---|---|---|---|---|---|---|
| | | | $N_2$ | butane | $N_2/SF_6$ | Butane/isobutane |
| 2 | 150 | 4 | 1200 | NA | 1.9 | NA |
| 2 | 150 | 7 | 11 | NA | 36 | NA |
| 2 | 150 | 16 | 4 | 0.19 | 611 | 4.6 |
| 2 | 150 | 16 | 5.7 | NA | 145 | NA |
| 2 | 150[a] | 7[a] | 3.8 | 1.9 | 610 | 80 |
| 2 | 150[a] | 7[a] | 12 | NA | 172 | NA |
| 0.4 | 150 | 16 | 0.50 | NA | 32 | NA |
| 0.4 | 150 | 16 | 0.96 | NA | 510 | NA |
| No seeds[b] | 175 | 16 | 6.7 | 3.5 | NA | 80 |
| No seeds[c] | 175 | 16 | 4 | 0.74 | NA | 92 |
| No seeds[d] | 180 | 24 | 40 | 10 | NA | 50 |
| No seeds[e] | 170 | 23 | 590 | 0.090 | 138 | 14 |

(a) Synthesized from a temperature profile, 130°C for 16 h, and immediately 150°C for 7 h.

(b) Synthesized without seeding at 175°C for 16 h, with a slightly different composition

(c) Permeation measurements at room temperature

(d) Literature results by Kusakabe et al. (1996)

(e) Literature results by Coronas et al. (1997).

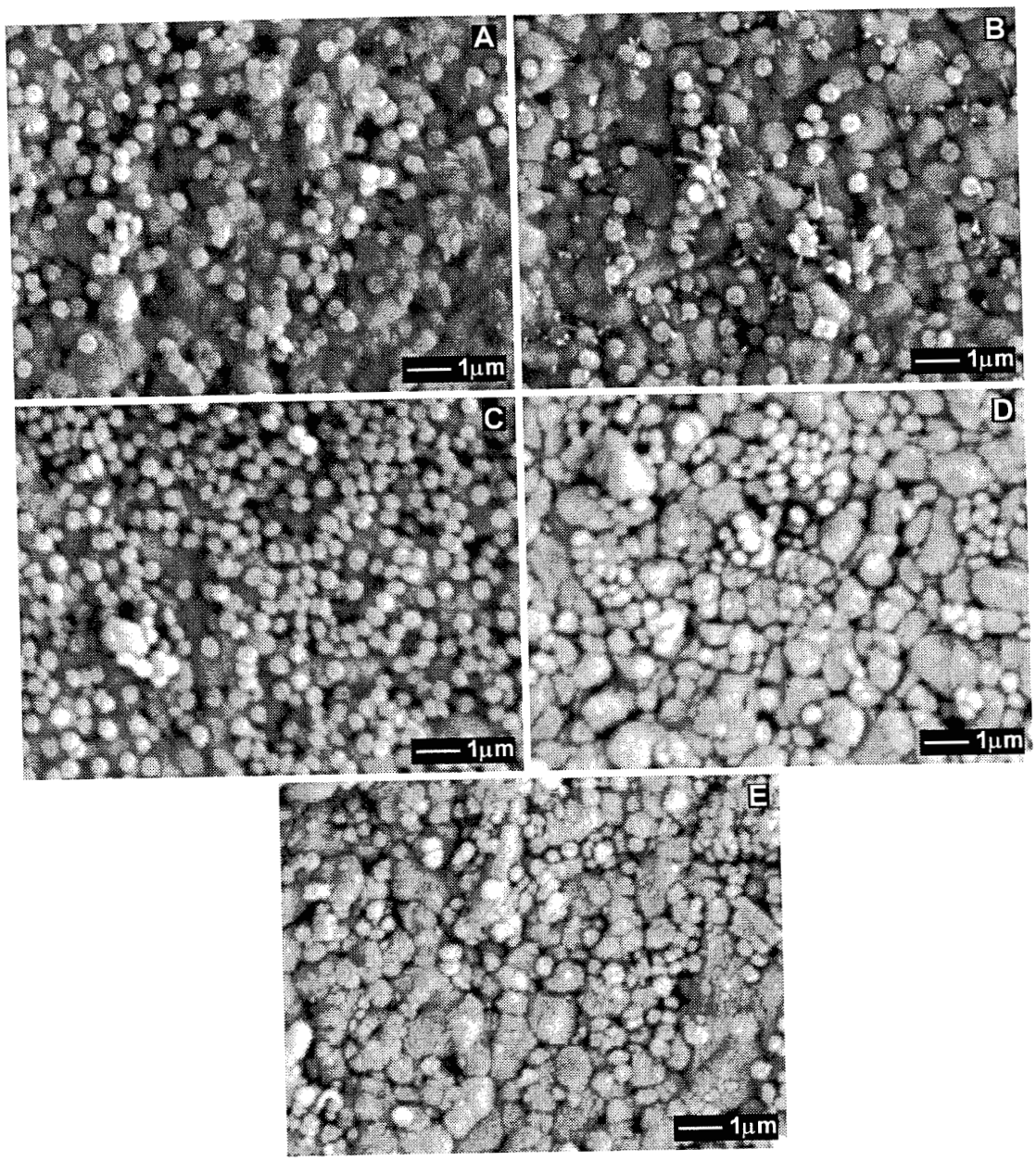


**Figure 3-1** Effect of pH on coating nonporous plates by 0.4 μm silicalite particles. (A) pH=10; (B) pH=9; (C) pH=8; (D) pH=7; (E) pH=5.8.

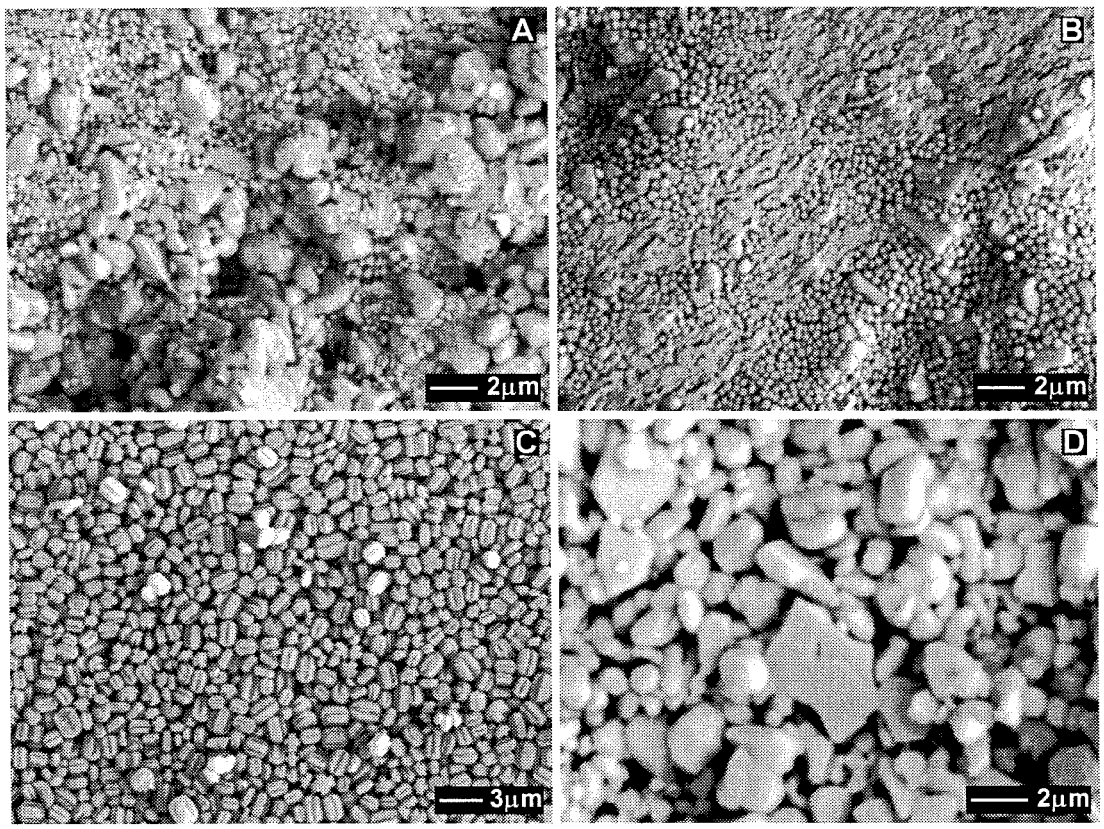


**Figure 3-2** Surface coating of a porous alumina tube by seeds of the size of 0.4 μm and 2 μm. (A) 0.4 μm at pH=5.8; (B) 0.4 μm at pH=8; (C) 2 μm at pH=8; (D) bare tube.

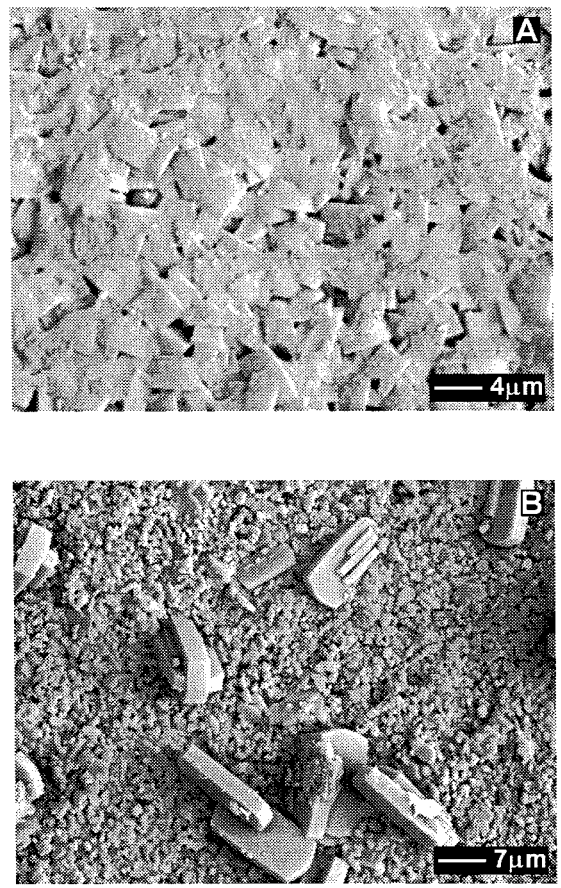


**Figure 3-3** Zeolite growth on a seeded (A) and unseeded (B) tube after 24 h hydrothermal reaction at 95°C.

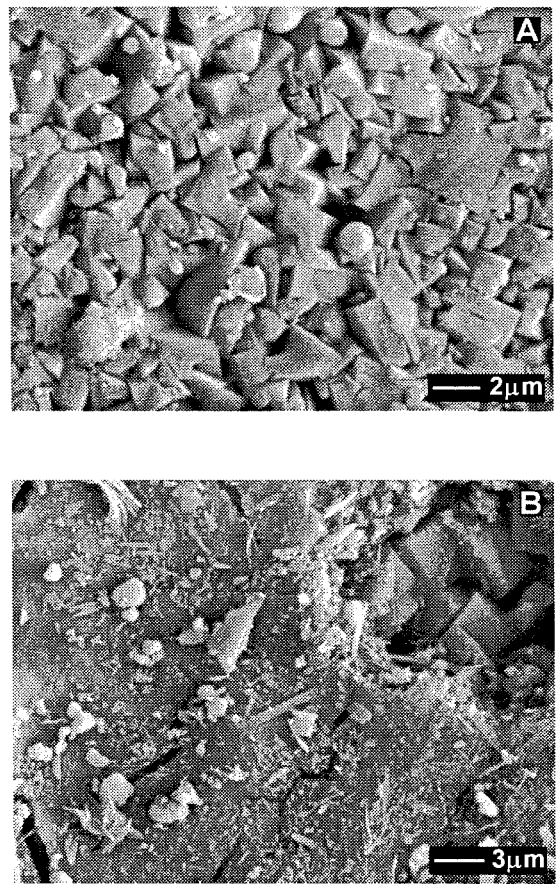


**Figure 3-4** Zeolite growth on a seeded (A) and unseeded (B) tube after 16 h hydrothermal reaction at 150°C.

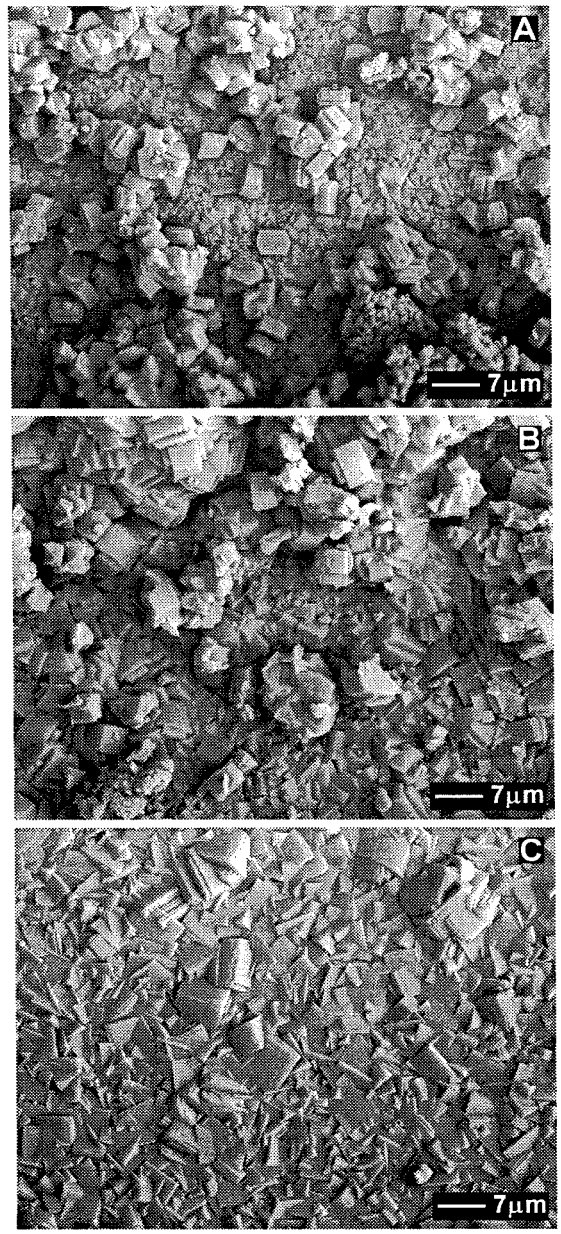


**Figure 3-5** Effect of NaOH content on membrane morphology. The synthesis solution compositions were $SiO_2$: 0.15TPABr: $x$NaOH: 98$H_2O$. (A) $x$=0.4; (B) $x$=0.5; (C) $x$=0.6.

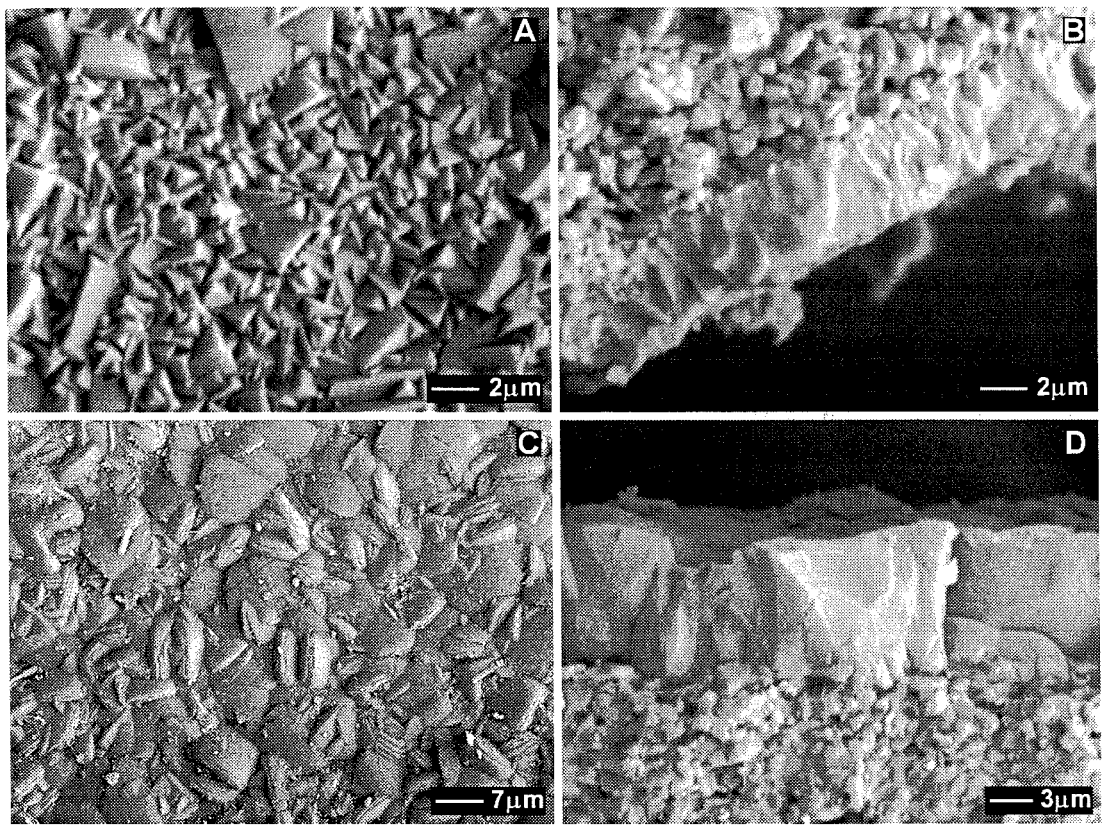


**Figure 3-6** SEM of zeolite films on tubes seeded by 0.4 μm particles after reaction for 12 h at 150°C (A,B) and on tubes seeded by 2 μm particles after reaction for 16 h at 150°C. (B) and (D) are cross-section views.

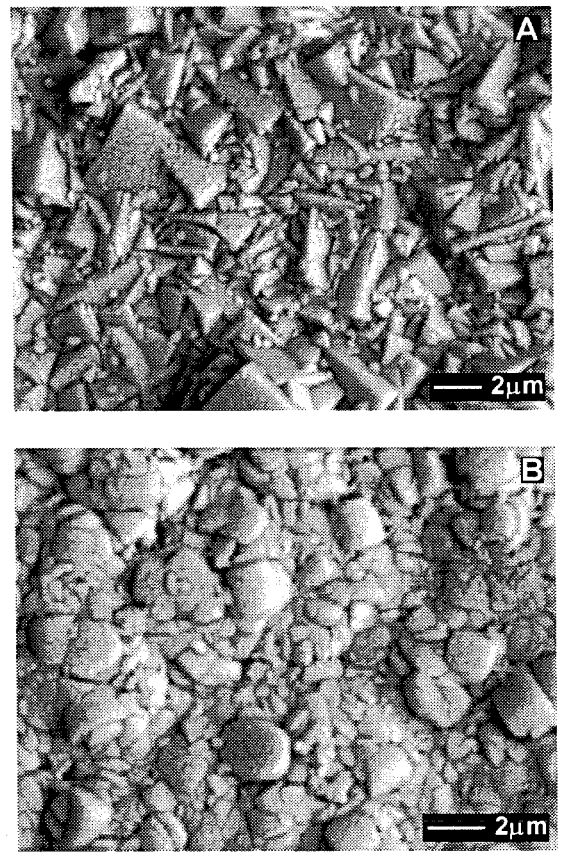


**Figure 3-7** SEM of zeolite films formed after reaction at 130°C for 20 h (A) and at 110°C for 23 h (B).

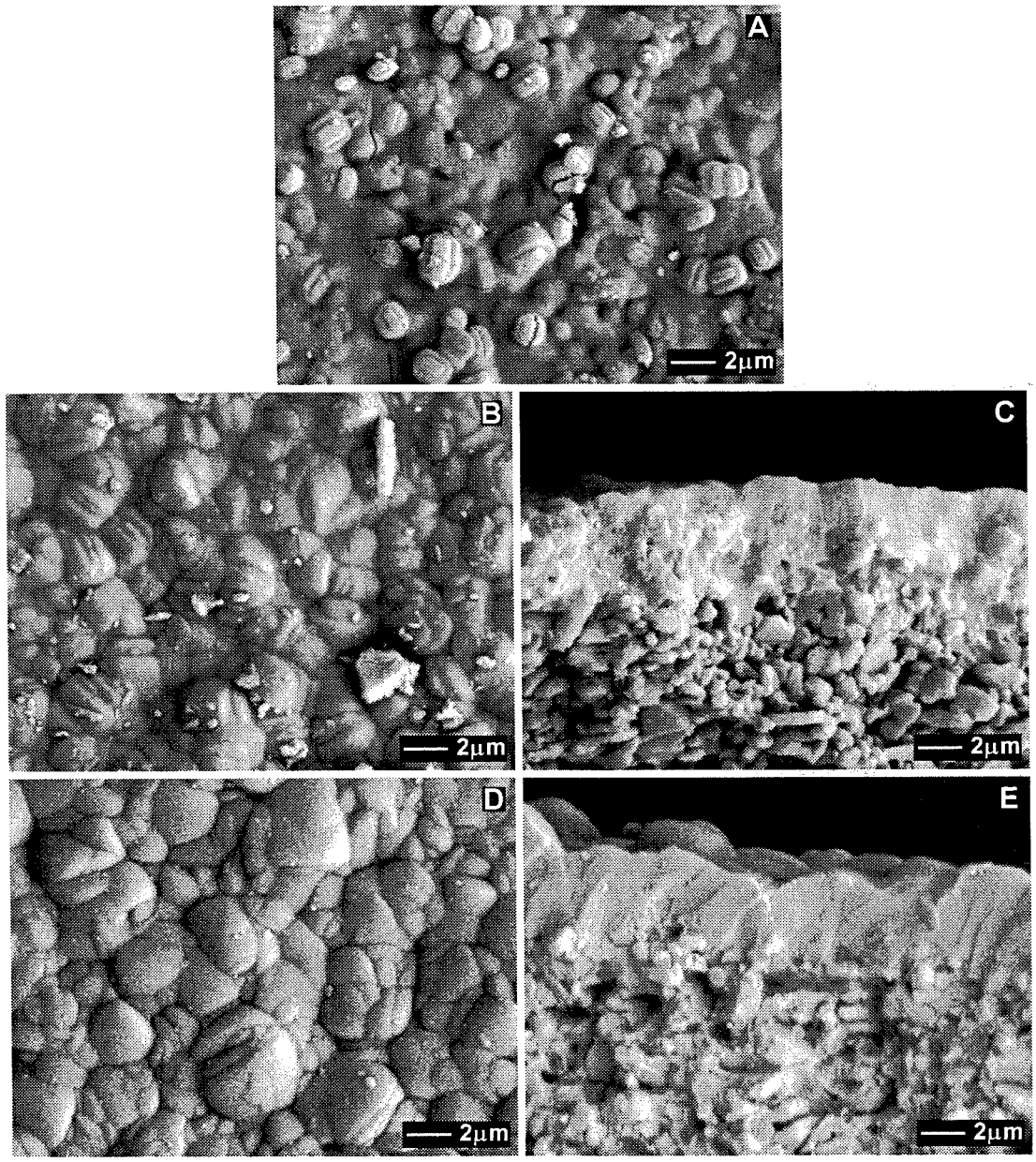


**Figure 3-8** SEM of zeolite films formed on porous tubes seeded with 2 μm particles after reaction at 150°C for different durations. (A) 2 h; (B, C) 4 h; (D, E) 7 h. The films after 16 h are shown in Fig. 6 (C, D).

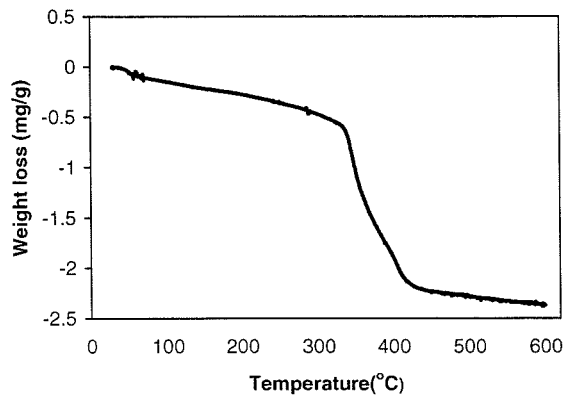


**Figure 3-9** TGA trace of a zeolite membrane deposited on a seeded tube.

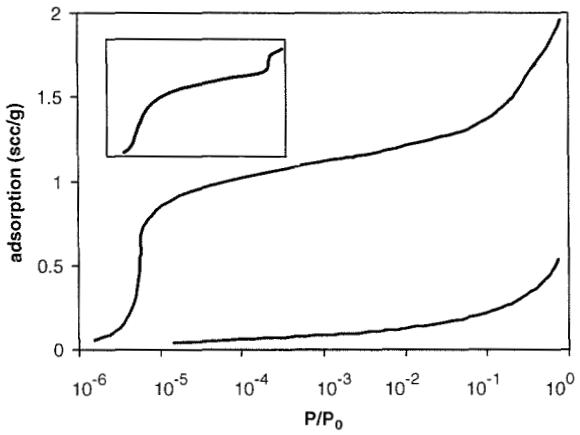


**Figure 3-10** Nitrogen adsorption isotherm of a zeolite membrane deposited on a seeded support before calcination (bottom curve) and after calcination (top curve). The insert is the $N_2$ adsorption isotherm of silicalite powder.

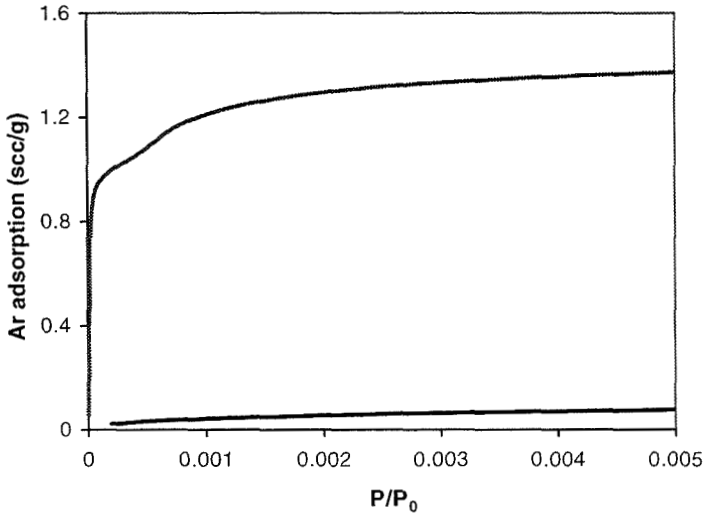


**Figure 3-11** Argon adsorption isotherm (77 K) of a ZSM-5 membrane deposited on a seeded support before calcination (bottom curve) and after calcination (top curve).

**Chapter 4**

# ZSM-5 Membrane Synthesis with Organic-Free Mixtures

Reprinted from *Microporous and Mesoporous Materials* (in print)

# ZSM-5 Membrane Synthesis with Organic-Free Mixtures

Re Lai and George R. Gavalas

*Division of Chemistry and Chemical Engineering, California Institute of Technology*

*Pasadena, California 91125*

## Abstract

Preparation of supported ZSM-5 membranes using a TPA-free synthesis gel was investigated. After exploring the effect of reaction mixture, the composition SiO2: $0.0125Al_2O_3$: $0.2675Na_2O$: $46H_2O$ was selected for membrane synthesis. Membranes were prepared by hydrothermal reaction on asymmetric $\alpha$-$Al_2O_3$ tubular supports. The membranes were characterized by SEM, EDS, XRD and Ar and $N_2$ adsorption. Permeation measurements with single gas and mixtures yielded selectivities for $H_2$ over *n*-butane above $10^4$ and for $O_2$ over $N_2$ 9-10. Permeation was strongly activated with the activation energies increasing sharply with molecular sizes.

## 4.1 Introduction

Much of the current research on zeolite membranes is focused on ZSM-5 or silicalite due to its ease of crystallization and high selectivity for hydrocarbon separations [1-9]. The synthesis protocols used to date for ZSM-5 or silicalite membranes have invariably employed $TPA^+$ (tetrapropylammonium) cations as templates. These organic

ions direct the structure formation by preorganizing silicate species into inorganic-organic composite structures and subsequently assembling these structures into crystalline ZSM-5 [10]. In this process, the $TPA^+$ molecules are occluded in the channel intersections of the as-synthesized ZSM-5 with the $C_4H_9$ arms extending into the straight and sinusoidal channels of the zeolite structure. Subsequent to the synthesis, calcination is needed to remove $TPA^+$ to access the pores. During this calcination $TPA^+$ decomposition, starting at *ca.* 350°C, results in abrupt shrinkage of the zeolite lattice yielding substantial stress that often results in microcracks in the zeolite film [11-13]. This difficulty may be eliminated by adoption of a $TPA^+$-free synthesis that not only renders calcination unnecessary, but also employs cheaper, less toxic reactants and allows easier waster disposal.

There have been several reports on ZSM-5 bulk synthesis based on organic-free approaches [14-18]. The crystallization field becomes much narrower when $TPA^+$ is not used. For example, while addition of aluminum is not required for the formation of ZSM-5 in the presence of $TPA^+$ cations, crystallization in the absence of $TPA^+$ is limited to a narrow range of aluminum concentration, with the $SiO_2/Al_2O_3$ ratio generally in the range of 40 to 180 [19]. Alternatively, ZSM-5 crystallization can be facilitated by organic additives, usually alcohols, ketones and amines, which play diverse roles as structure-directing agents, void fillers, host crystal stabilizers, and gel chemistry modifiers [20-26].

Recently, Mintova et al. reported the preparation of ZSM-5 films from a reaction mixture free of organics [27]. As nonporous substrates were used therein, permeation properties were not available. Here we report preparation of ZSM-5 membranes on

porous alumina tubes without the aid of $TPA^+$ templates. Synthesis was carried out using small organic additives and under completely organic-free conditions. To ensure the crystallization of ZSM-5 phase, surface seeding was used in all cases [9].

## 4.2 Experimental

The synthesis mixture was prepared by dissolving a measured amount of $Al_2(SO_4)_3 \cdot 18H_2O$ (Aldrich) in NaOH solution. Colloidal silica (Ludox SM-30, Aldrich), filtered using a Buchner funnel with a coarse fritted disc, was added to the solution dropwise under stirring. In some experiments the hydrogel was aged under stirring at room temperature for 1 day.

Asymmetric $\alpha$-$Al_2O_3$ tubes (Inocermic, 60nm at OD) and non-porous alumina plates (Intertec Southwest) were used as supports. They were cleaned by boiling in acetone for 10 min., and heated in air at 600°C for 5 h before use. Coating the tube surface with a layer of TPA-silicalite seeds, of about 0.4 μm size, followed our previous protocol [9] with the exception that ultrasonication was omitted. The seeded tubes were then calcined at 550°C for 5 h. Hydrothermal reaction was carried out in a preheated oven at 180°C for a specified period, with the support held vertically in a Teflon-lined autoclave.

Those membranes tested for permeation properties were prepared using two hydrothermal reaction cycles. The first hydrothermal synthesis was conducted at 180°C for 8 h. The tube was then taken out, washed with water, dried in air, and subsequently

underwent the second hydrothermal treatment at 180°C for 16 h. Afterwards, the tube was washed, soaked in water for 1 day, dried in air, and mounted on glass tubing by epoxy resin (Torr seal, Varian). The tube was heated under vacuum at 160°C overnight before permeation measurements. Single gas permeation was conducted by the pressure rise method [3]. Permeation measurements for gas mixtures were carried out using a gas chromatograph with a thermal conductivity detector (SRI 1000) using Ar as the sweep gas and the carrier gas.

Scanning electron microscopy (SEM) was used to examine the morphology of the membranes. Characterization of the ZSM-5 film grown on alumina plates included XRD (Cu-$K_\alpha$) to confirm the phase of the film, and Ar and $N_2$ adsorption at 77 K using an ASAP 2010 porosimeter (Micromeritics). The as-synthesized sample was soaked in water for 1 day, dried, and degassed at 300°C before the adsorption measurement.

## 4.3 Results and discussion

### *Effects of gel composition*

A range of composition was explored to find suitable film growth conditions. Surface zeolitization was found to be facilitated by organic additives, acetone, EtOH or *n*-PrOH, whose use was based on the consideration that they could be removed from ZSM-5 pores by evacuation without calcination. The effect of these additives, however, was only important when aging of the hydrogel was not employed. When the reaction mixture underwent aging at room temperature for 1 day, surface crystallization was

greatly accelerated and use of organic additives was not anymore necessary as zeolitization enhancers.

Film growth at different NaOH concentrations is presented Fig. 1. The effects of NaOH on zeolite crystallization are diverse. In the absence of organic cations, $Na^+$ functions as the structure directing species in zeolitization [19]. Alkalinity furthermore has multifaceted effects on $TPA^+$-free synthesis [16,25,28]. Increase of alkalinity expedites the dissolution of the gel phase, which in turn facilitates formation of reactive species. Alkalinity is also known to favor crystallite intergrowth in bulk synthesis. Meanwhile, at high alkalinity redissolution of the crystallites also takes place. Combination of all these factors limits the conditions of film growth to a narrow range. The experiments summarized in Fig. 1 show the crystallite intergrowth improving with increasing alkalinity but when the $NaOH:SiO_2$ ratio reached 0.6, XRD-amorphous material was formed on top of the support tube.

Variation of the aluminum content was further used to manipulate the membrane morphology (Fig. 2). Increasing the aluminum content was found to promote the intergrowth of adjacent crystals, in accordance to what is known in bulk synthesis [25]. Kinetically, aluminate has been reported to accelerate ZSM-5 crystallization in template-free systems [16,25], opposite to the general trend under $TPA^+$-containing conditions [29-32]. The useful ratios of $SiO_2/Al_2O_3$ for ZSM-5 synthesis in the absence of $TPA^+$ were reported to be in the range of 40 to 180, much narrower than those in $TPA^+$-containing synthesis. The film prepared using the composition

$SiO_2$: 0.2675$Na_2O$: 0.0125$Al_2O_3$: 46$H_2O$

consists of a continuous layer of well intergrown zeolitic crystallites as shown in Fig. 2b. This composition was used for further experiments.

***Characterization***

Figure 3 shows SEM of a membrane cross section. Formed on the asymmetric support was a 5-6 μm zeolite film of Si:Al about 15, as estimated by EDS. This ratio is much lower than the bulk ratio of 80. Enrichment of alumina in the zeolite product has been observed previously in both bulk and film synthesis of ZSM-5 [19,32,33]. It is noteworthy that the Si:Al ratio of the film of Fig. 3 is much lower than the 100-200 ratio usually measured for films prepared with the aid of $TPA^+$ [32,33].

X-ray diffraction was used to verify the phase of the zeolite layer prepared on an alumina plate. The XRD pattern is shown in Fig. 4, in juxtaposition with the XRD theoretical standard of randomly-oriented calcined ZSM-5. Diffraction confirms that the zeolite layer is textured ZSM-5, as expected for seeded growth [7,27].

High-resolution Ar adsorption measurements clearly indicate the microporous nature of the zeolite film (Fig. 5). The adsorption isotherm exhibits a step at $P/P_0=10^{-4}$ that is characteristic of argon adsorption in ZSM-5 or silicalite, corresponding to the adsorbate phase transition from a less ordered one to an ordered one [34-36]. The step is quite diffuse here owing to the high alumina content [35].

The $N_2$-BET specific surface area of the zeolite film grown on the alumina plate is 329 $m^2/g$, in good agreement with other literature reports on ZSM-5 prepared without organic additives [16,27], but somewhat lower than the surface areas of ZSM-5 prepared using $TPA^+$ [37,38]. The lower surface area was suggested to be due to occlusion of amorphous species inside the zeolitic pores [16].

***Permeation measurements***

Three membranes were prepared on asymmetric alumina tubes using the composition $SiO_2$: $0.2675Na_2O$: $0.0125Al_2O_3$: $46H_2O$. Their permeation properties are summarized in Table 1. All of these membranes display selectivities that strongly depend on the kinetic molecular sizes. At room temperature, the ideal selectivities of $H_2$ over *n*-butane are above $10^4$, and those of $O_2$ over $N_2$ are 9-10. These selectivities compare favorably with literature results of membranes prepared with $TPA^+$, suggesting that the TPA-free membrane synthesis indeed can be used to prepare membranes largely free of defects. Permeation measurements for mixtures of hydrogen with nitrogen or methane (Table 2) gave mixture selectivities similar to the single gas selectivities. This agreement reflects the fact that $N_2$, $CH_4$ and $H_2$ are not strongly adsorbed at the measurement temperature [39-41] so that pore blocking by the slowly moving species is not encountered. On the other hand, these membranes did not possess selectivity for *n*-butane-*iso*-butane separation. Previous studies report ZSM-5 or silicalite membranes with selectivities of *n*-butane over *iso*-butane ranging from 0.3 up to 80. The lack of *n*-butane-*iso*-butane separation of the present membranes is probably due to their different adsorptive properties.

Permeation of the membranes herein is highly activated even for small molecules like $H_2$, $N_2$ and $CH_4$, and as can be seen from Table 1, the activation energy increases with the molecular size, indicative of a kinetic origin. These membranes differ from others that exhibit little temperature dependence for permeation of single gases $H_2$, $N_2$ and $CH_4$ [1,3-6,8], but resemble those reported by Lovallo et al. [7,42]. Permeation across zeolite membranes generally has two components, activated intracrystalline diffusion and diffusion through non-zeolitic defects that usually displays little temperature dependence [43,44]. Van de Graaf et al. found that after excluding the contribution from non-zeolitic defects, the permeances of He and Ne across a silicalite membrane were highly activated above room temperature [44]. Thus, the high activation energy of permeation of the membranes listed in Table 1 indicates the preponderance of intrazeolitic diffusion. The intracrystalline barrier to diffusion is generally due to the difference between the potential energy of a molecule inside a channel and in an intersection [45]. For the ZSM-5 membranes prepared by the $TPA^+$-free approach, occlusion of amorphous species inside the channel structure suggested by the adsorption measurements may raise further that energy barrier. There are also other possible causes of the high activation energy such as surface barriers [46-50], lattice faults and structural defects [51].

## 4.4 Conclusions

ZSM-5 membranes were prepared on asymmetric porous alumina supports without the use of organic templates. The membranes have Si/Al ratios much higher than

membranes prepared using $TPA^+$ in the synthesis mixture. Gas permeation measurements yielded high selectivities based on molecular size. At room temperature, the selectivites of $H_2$ over $N_2$ and over n-butane were 500 and $10^4$, respectively. The permeation across the membranes was highly activated, suggestive of occlusion of amorphous material inside the zeolite channels.

## Acknowledgement

This study was funded by a grant from NSF and by Chevron Research and Technology Co.

## References

[1] E.R. Geus, M.J. den Exter and H. van Bekkum, J. Chem. Soc.-Faraday Trans. 88 (1992) 3101.

[2] M.D. Jia, B.S. Chen, R.D. Noble and J.L. Falconer, J. Membr. Sci. 90 (1994) 1.

[3] Y.S. Yan, M.E. Davis and G.R. Gavalas, Ind. Eng. Chem. Res. 34 (1995) 1652.

[4] Z. Vroon, K. Keizer, M.J. Gilde, H. Verweij and A.J. Burggraaf, J. Membr. Sci. 113 (1996) 293.

[5] W.J.W. Bakker, F. Kapteijn, J. Poppe and J.A. Moulijn, J. Membr. Sci. 117 (1996) 57.

[6] K. Kusakabe, S. Yoneshige, A. Murata and S. Morooka, J. Membr. Sci. 116 (1996) 39.

[7] M.C. Lovallo and M. Tsapatsis, AICHE J. 42 (1996) 3020.

[8] J. Coronas, J.L. Falconer and R.D. Noble, AICHE J. 43 (1997) 1797.

[9] R. Lai and G.R. Gavalas, Ind. Eng. Chem. Res. 37 (1998) 4275.

[10] S.L. Burkett and M.E. Davis, J. Phys. Chem. 98 (1994) 4647.

[11] E.R. Geus and H. Van Bekkum, Zeolites 15 (1995) 333.

[12] M.J. den Exter, H. van Bekkum, C.J.M. Rijn, F. Kapteijn, J.A. Moulijn, H. Schellevis and C.I.N. Beenakker, Zeolites 19 (1997) 13.

[13] X. Lin, J.L. Falconer and R.D. Noble, Chem. Mat. 10 (1998) 3716.

[14] J.M. Berak and R. Mostowicz, Stud. Surf. Sci. Catal. 24 (1985) 47.

[15] R. Aiello, F. Crea, A. Nastro and C. Pellegrino, Zeolites 7 (1987) 549.

[16] V.P. Shiralkar and A. Clearfield, Zeolites 9 (1989) 363.

[17] F.Y. Dai, M. Suzuki, H. Takahashi and Y. Saito, In M.L. Occelli and H.E. Robson (Ed.), Zeolite Synthesis, ACS, Washington, D.C., 1989, pp. 244.

[18] W. Schwieger, K.-H. Bergk, D. Freude, M. Hunger and H. Pfeifer, In M.L. Occelli and H.E. Robson (Ed.), Zeolite Synthesis, ACS, Washington, D.C., 1989, pp. 274.

[19] R. Szostak, Molecular Sieves: Principles of Synthesis and Identifications, Van Nostrand Reinhold, New York, 1989.

[20] B.M. Lok, T.R. Cannan and C.A. Messina, Zeolites 3 (1983) 282.

[21] R.M. Barrer, Stud. Surf. Sci. Catal. 24 (1985) 1.

[22] A. Araya and B.M. Lowe, Zeolites 6 (1986) 111.

[23] S. Schwarz, M. Kojima and C.T. Oconnor, Appl. Catal. 73 (1991) 313.

[24] E. Narita, K. Sato, N. Yatabe and T. Okabe, Ind. Eng. Chem. Prod. Res. Dev. 24 (1985) 507.

[25] M.A. Uguina, A. Delucas, F. Ruiz and D.P. Serrano, Ind. Eng. Chem. Res. 34 (1995) 451.

[26] T. Mole and J.A. Whiteside, J. Catal. 75 (1982) 284.

[27] S. Mintova, J. Hedlund, V. Valtchev, B.J. Schoeman and J. Sterte, J. Mater. Chem. 8 (1998) 2217.

[28] E.J.P. Feijen, J.A. Martens and P.A. Jacobs, Stud. Surf. Sci. Catal. 84 (1994) 3.

[29] G. Golemme, A. Nastro, J.B. Nagy, B. Subotic, F. Crea and R. Aiello, Zeolites 11 (1991) 776.

[30] A.E. Persson, B.J. Schoeman, J. Sterte and J.E. Otterstedt, Zeolites 15 (1995) 611.

[31] A. Iwasaki, T. Sano and Y. Kiyozumi, Microporous Mesoporous Mat. 25 (1998) 119.

[32] R. Lai, Y. Yan and G.R. Gavalas, Micropor. Mesopor. Mat. 37 (2000) 9.

[33] Y.H. Yan, M. Tsapatsis, G.R. Gavalas and M.E. Davis, J. Chem. Soc.-Chem. Commun. (1995) 227.

[34] U. Muller, K.K. Unger, D. Pan, A. Mersmann, Y. Grillet, F. Rouqerol and J. Rouqerol, Stud. Surf. Sci. Catal. 46 (1989) 625.

[35] P.L. Llewellyn, J.P. Coulomb, Y. Grillet, J. Patarin, H. Lauter, H. Reichert and J. Rouquerol, Langmuir 9 (1993) 1846.

[36] R.J.-M. Pellenq and D. Nicholson, Stud. Surf. Sci. Catal. 87 (1994) 21.

[37] I.D. Harrison, H.F. Leach and D.A. Whan, In D. Olson and A. Bisio (Ed.), Proceedings of the Sixth International Zeolite Conference: Reno, USA 10-15 July 1983, Butterworths, Guildford, Surrey, UK, 1984, pp. 479.

[38] A. Gervasini, Appl. Catal. A-Gen. 180 (1999) 71.

[39] H.B. Abdul-Rehman, M.A. Hasanain and K.F. Loughlin, Ind. Eng. Chem. Res. 29 (1990) 1525.

[40] L.V.C. Rees, In G. Öhlmann, H. Pfeifer and R. Fricke (Ed.), Catalysis and Adsorption by Zeolites, Elsevier, Amsterdam, 1991, pp. 61.

[41] V.R. Choudhary and S. Mayadevi, Zeolites 17 (1996) 501.

[42] M.C. Lovallo, A. Gouzinis and M. Tsapatsis, AICHE J. 44 (1998) 1903.

[43] J.C. Poshusta, R.D. Noble and J.L. Falconer, J. Membr. Sci. 160 (1999) 115.

[44] J.M. van de Graaf, F. Kapteijn and J.A. Moulijn, Chem. Eng. Sci. 54 (1999) 1081.

[45] J.R. Xiao and J. Wei, Chem. Eng. Sci. 47 (1992) 1123.

[46] E.G. Derouane, L. Leherte, D.P. Vercauteren, A.A. Lucas and J.M. Andre, J. Catal. 119 (1989) 266.

[47] R.M. Barrer, J. Chem. Soc.-Faraday Trans. 86 (1990) 1123.

[48] F. Vignemaeder, S. Elamrani and P. Gelin, J. Catal. 134 (1992) 536.

[49] D.M. Ford and E.D. Glandt, J. Phys. Chem. 99 (1995) 11543.

[50] M. Bulow and A. Micke, Adsorpt.-J. Int. Adsorpt. Soc. 1 (1995) 29.

[51] E.R. Geus, J.C. Jansen and H. Van Bekkum, Zeolites 14 (1994) 82.

[52] D.W. Breck, Zeolite Molecular Sieves, Robert E Kreiger Publishing Company, Malabar, Florida, 1984.

**Table 4-1** Single gas permeances and activation energies of permeation of ZSM-5 membranes.

| Permeation Temperature | Permeance ($10^{-10}$ mol/Pa $m^2$ s) | | | | | | | | |
|---|---|---|---|---|---|---|---|---|---|
| | $H_2$ (2.89) | $CO_2$ (3.3) | $O_2$ (3.46) | $N_2$ (3.64) | $CH_4$ (3.8) | $SF_6$ (5.5) | n-butane (4.3) | i-butane (5.0) | kin.dia.(Å)[52] |
| 298 K | 67 | 51 | 1.3 | 0.14 | 0.066 | <0.006 | <0.004 | -- | Membrane A (This work) |
| 423 K | 1200 | 81 | 46 | 11 | 5.2 | 0.025 | 0.10 | 0.15 | |
| $E_a$ (kJ/mol) | 24 | 23 | 30 | 36 | 37 | -- | -- | -- | |
| 298 K | 29 | 1.4 | 0.58 | 0.056 | 0.034 | -- | <0.0095 | -- | Membrane B (This work) |
| 423 K | 1100 | 130 | 60 | 17 | 9.6 | <0.009 | 0.090 | -- | |
| $E_a$ (kJ/mol) | 31 | 38 | 39 | 48 | 47 | -- | -- | -- | |
| 423 K | 610 | 61 | 29 | 8.5 | 6.4 | -- | 0.68 | -- | Membrane C (This work) |
| 423 K | 1230 | -- | 62 | 20 | -- | -- | 35 | 18 | Lovallo et al. [7] |
| $E_a$ (kJ/mol) | 11 | | 32 | 26 | -- | -- | -- | -- | |
| 373 K | 260 | 55 | 17 | 8.0 | 9.0 | -- | -- | -- | Lovallo et al. [42] |
| $E_a$ (kJ/mol) | 16 | 26 | 30 | 24 | 22 | -- | -- | -- | |
| 373 K | -- | 1600 | -- | 350 | 810 | -- | 1200 | 73 | Kusakabe et al. [6] |
| $E_a$ (kJ/mol) | -- | 4.4 | -- | 3.2 | 3.5 | -- | -- | 20 | |
| 423 K | 21300 | 6080 | -- | 5850 | -- | -- | 1040 | 3400 | Coronas et al. [8] |
| $E_a$ (kJ/mol) | 2.3 | 1.9 | -- | 1.2 | -- | -- | 17 | 18 | |
| 458 K | 1010 | 739 | 410 | 402 | 734 | -- | 585 | 18.8 | Yan et al. [3] |
| $E_a$ (kJ/mol) | 3.7 | -1.3 | 0.81 | 1.8 | 5.0 | -- | 15 | 11 | |
| 418 K | 940 | 270 | 240 | 210 | 250 | -- | -- | -- | Geus et al. [1] |
| $E_a$ (kJ/mol) | 1.1 | -1.4 | -- | -2.1 | -3.5 | -- | -- | -- | |

**Table 4-2** Permeaces ($10^{-10}$ mol/Pa $m^2$ s) for $H_2$-($N_2$,$CH_4$) mixtures across Membrane B at 423 K.

| B | Feed gas (atm.) | | Permeaces | | Selectivity |
|---|---|---|---|---|---|
| | $H_2$ | B | $P_{H2}$ | $P_B$ | $P_{H2}/P_B$ |
| $N_2$ | 0.018 | 0.982 | 260 | 6.8 | 38 |
| $CH_4$ | 0.31 | 0.69 | 330 | 5.4 | 61 |

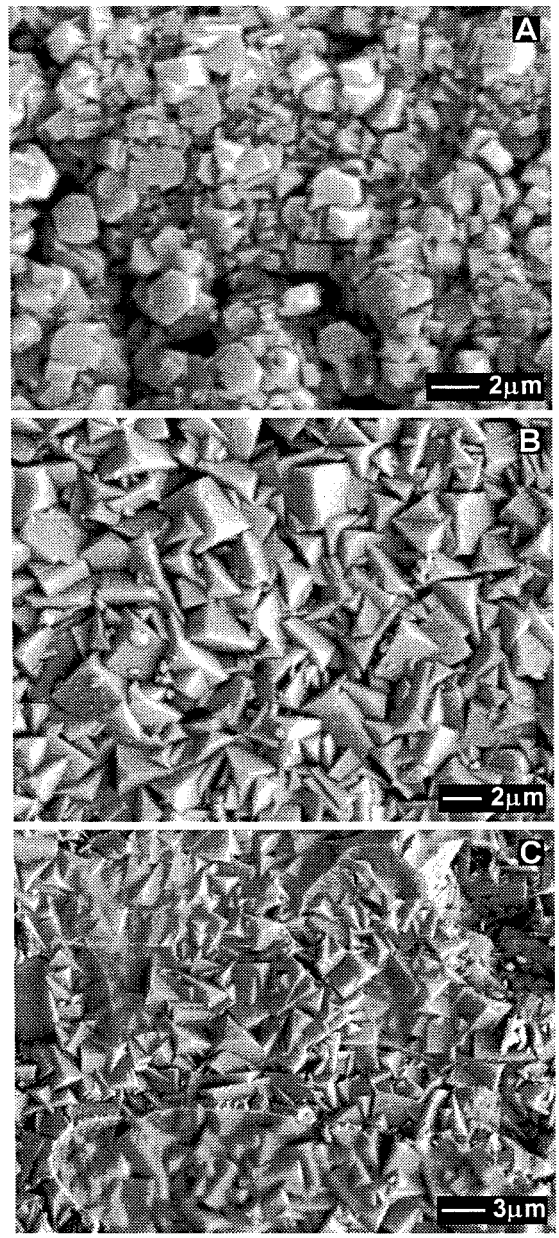


**Figure 4-1** Effect of NaOH on zeolite film morphology. The reaction gel aged 1 d under stirring at room temperature. Hydrothermal synthesis was conducted at 180°C for 16 h. The synthesis mixture was of composition $SiO_2$: $x$NaOH: $0.01Al_2O_3$: $46H_2O$, where (A) $x$=0.5; (B) $x$=0.535; (C) $x$=0.6.

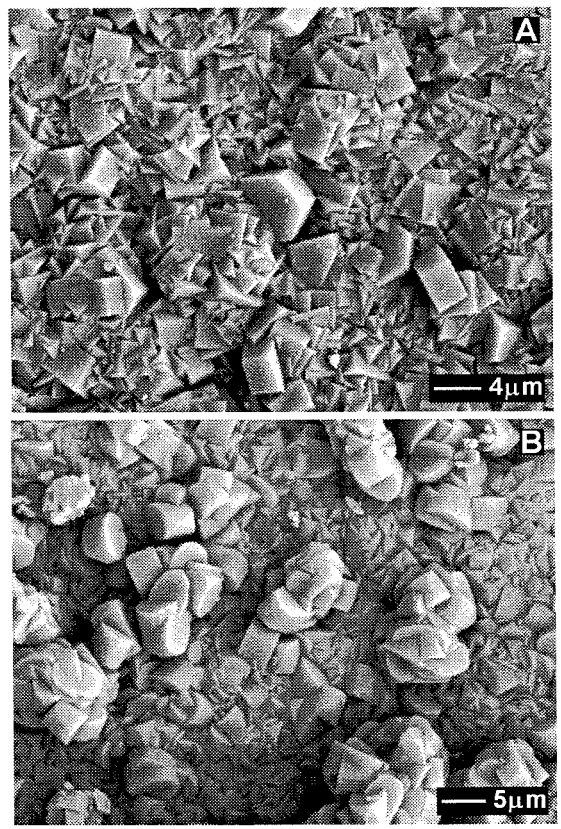


**Figure 4-2** Effect of aluminum on zeolite film morphology. The reaction gel aged 1 d under stirring at room temperature. Hydrothermal synthesis was conducted at 180°C for 16 h. The synthesis mixture was of composition $SiO_2$: 0.54NaOH: $xAl_2O_3$: $46H_2O$, where (A) $x$=0.0083; (B) $x$=0.0125. Refer to Fig. 1b for $x$=0.01.

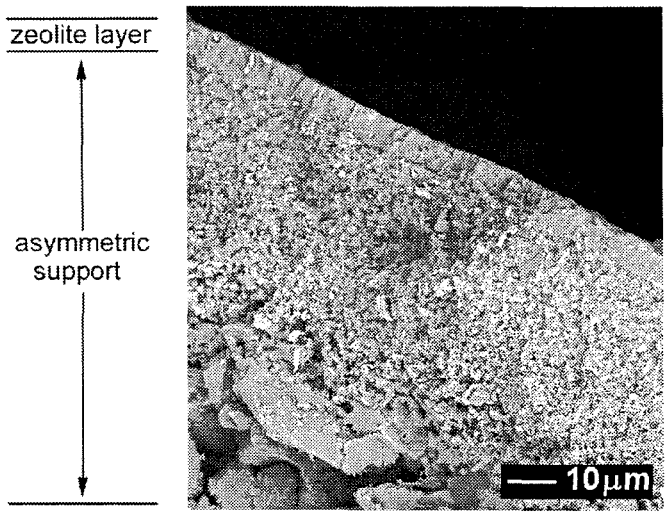


**Figure 4-3** Cross section of the ZSM-5 membrane grown on the asymmetric alumina support. The reaction mixture was of composition $SiO_2$: 0.535NaOH: $0.0125Al_2O_3$: $46H_2O$. The membrane was prepared by two cycles of hydrothermal treatment, the first 8 h and the second 16 h at 180°C.

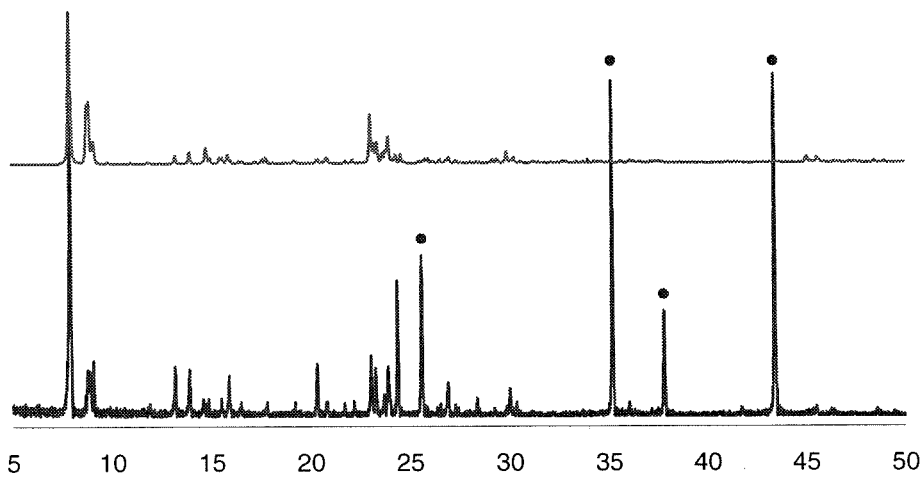


**Figure 4-4** XRD pattern of a zeolite film prepared on an alumina plate by the organic-free method at 180°C for 21 h. The dotted peaks correspond to the α-$Al_2O_3$ substrate. The top curve represents the theoretical standard of calcined silicalite with random orientation.

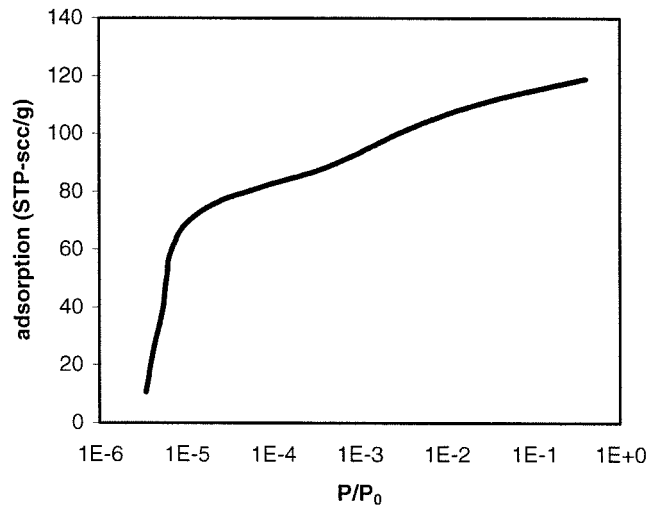


**Figure 4-5** Ar adsorption (77K) of a ZSM-5 film prepared on an alumina plate by the organic-free method at 180°C for 21 h.

Chapter 5

# Parallel Synthesis of ZSM-5 Zeolite Films from Clear Organic-Free Solutions

# Parallel Synthesis of ZSM-5 Zeolite Films from Clear Organic-Free Solutions

Re Lai, Beom-Seok Kang and George R. Gavalas

*Division of Chemistry and Chemical Engineering, California Institute of Technology*

*Pasadena, California*

## Abstract

Parallel synthesis of supported zeolite films was conducted in a reactor consisting of 21 wells drilled into a Teflon block and capped by a nonporous alumina disk serving as the substrate. The Teflon-alumina assembly was compressed in a Parr bomb and placed in an oven with the disk in a horizontal or vertical orientation. After synthesis the films formed on the alumina disk as nonoverlapping circular spots were characterized by SEM, EDS, and XRD. The morphology and X-ray pattern of the films is compared with those of films grown in a conventional autoclave reactor. An array of 20 films was prepared on a seeded disk to study the effect of alkalinity and Si/Al ratio in growth from template-free clear solutions. The composition range $SiO_2$: (0.5-0.7)NaOH: (1/300-1/700)$Al_2O_3$: 80$H_2O$ yielded continuous ZSM-5 films of Si/Al~20.

## 5.1 Introduction

High throughput synthesis and screening ("combinatorial") techniques have been recently introduced to the discovery and optimization of solid-state materials [1-3], such as phosphors [4], superconductors [5], dielectrics [6] and heterogeneous catalysts [7-11]. In this study parallel synthesis is applied to prepare supported ZSM-5 zeolite films. Identifying compositions that produce a microscopically continuous zeolite film usually constitutes the first step in zeolite membrane synthesis [12,13], an area that has attracted considerable interest in the last decade due to the prospective gas separation applications [13-17]. Zeolite films are also of interest for sensor and non-linear optical material applications [18,19]. As zeolite film synthesis is known to be able to manipulate the film thickness, composition and even crystallite orientation [19-22], it offers an interesting and powerful approach to prepare supported zeolite arrays intended as catalytic libraries.

There are several reports on the parallel synthesis of zeolite powders [23-25]. Akporiaye and coworkers manually removed zeolite powder precipitates from the autoclave micro-wells and characterized them by X-ray diffraction (XRD) [23]. Other groups employed post-synthetic treatment to attach the powder products to a silicon wafer or filter paper in order to eliminate the need for individual sample handling. X-ray micro-diffraction was then used to identify individual sample members. Klein et al. used a silicon wafer as the bottom of a multi-well autoclave [24]. After reaction, the precipitates were heated to bond them to the wafer. They also used this method to produce zeolite libraries for catalytic investigation [26]. Bein and coworkers designed a

centrifuge apparatus that allowed quantitative product recovery onto filter paper without manipulation of individual samples [25].

In this study the parallel synthesis was applied to explore ZSM-5 film growth in organic-free clear synthesis solutions. Compared to the standard ZSM-5 synthesis that involves organic $TPA^+$, the organic-free synthesis employs chemicals of lower cost and toxicity. More importantly from the standpoint of film or membrane synthesis, it renders unnecessary the calcination employed to remove the $TPA^+$ molecules, during which lattice changes often produce microcracks in the zeolite films [27-30].

Clear solutions containing organic templates have been widely used in ZSM-5 membrane synthesis, but organic-free synthesis of ZSM-5 in either powder [31-33] or film [34] form invariably employed hydrogel reaction mixtures. Clear solution allows easy product separation in ZSM-5 powder synthesis and has therefore been quite popular in mechanism investigations. Clear solutions are also desirable in film preparation to prevent spatial inhomogeneities. In this paper, after examining some operational details we apply parallel synthesis to the growth of ZSM-5 films from clear, organic-free solutions.

## 5.2 Experimental

### *Synthesis Solutions*

All chemicals were purchased from Aldrich unless specified otherwise. First, a 25wt.% tetrapropylammonium bromide (TPABr) solution was prepared and filtered with

0.45 μm cellulose acetate membranes (Corning). Two types of silicon sources were used: sodium silicate solution (14% NaOH and 27% $SiO_2$), and tetraethylorthosilicate (TEOS). Sodium silicate was filtered using a Buchner funnel with a coarse fritted disc immediately before use. When TEOS was used as the silicon source, it was first dissolved in tetraproprylammonium hydroxide (TPAOH) to form a clear solution of composition TEOS: 0.15TPAOH: 0.7NaOH: $98H_2O$, which was then filtered before use with a PTFE filter (0.45 μm, VWR).

The synthesis mixture was prepared by mixing a measured amount of chemicals in a transparent LDPE vial of volume 1 mL (Nalgene). When sodium silicate solution was used, $H_2SO_4$ (5N, VWR) was added to adjust alkalinity of the final solution. After thorough shaking, a clear synthesis solution was formed and aged at room temperature for one day without stirring. Occasionally, the synthesis mixtures turned turbid immediately after mixing, but the solution became clear after standing for several hours.

***Substrates***

The substrates employed were nonporous alumina disks ($\alpha$-$Al_2O_3$, Coors Ceramics), 1 inch in diameter, chosen to fit in the sample holder of the scanning electron microscope (SEM). The substrates were cleaned by ultrasonication in acetone for 10 min., and treated with an oxidizing solution of 70 vol% $H_2O$, 15 vol% $H_2O_2$ (30%) and 15 vol% $NH_3$ (25%) at 80°C for 10 min. [22,35].

Seeding was used as in an earlier study [34] to facilitate growth of ZSM-5 films from organic-free solutions. Seeding of the alumina disks was carried out using a previously developed protocol [12,34]. Briefly, 0.33 wt% silicalite particles of approximately 0.4 μm size were dispersed in pH=8 buffer solution. The substrate was immersed in the seeding solution, dried, washed with water, and subsequently calcined at 550°C for 5 h. The pH value of 8 was chosen to facilitate coating by maintaining opposite charge on the alumina surface and silicalite particles.

***Multi-Well Reactor***

Parallel synthesis was carried out in a multi-well reactor similar to that used in reference [24]. The reactor is shown schematically in Figure 1. It contains twenty-one wells of approximately 3 mm diameter and 5 mm depth drilled in a Teflon block. After introducing the solutions, the wells were capped by the alumina disk substrate and enclosed in a Parr reaction bomb, with the substrate firmly pressed against the Teflon block to seal all wells. The volume of solution in each well was 35 μL, a little less than the 40 μL volume of the wells. To ensure full contact of the substrate with the solution, the bomb was inverted and gently shaken several times with the substrate at the bottom of the solution and then placed in the oven in one of two orientations: either with the substrate horizontally at the bottom of the synthesis solution, or rotated by 90° fixing the substrate in a vertical position. After reaction, the zeolite films in all wells were found firmly attached to the substrate.

*Characterization*

The morphology of the films in the array was examined by scanning electron microscopy (SEM, Camscan 15 kV), and their elemental composition was estimated by energy dispersive spectroscopy (EDS). X-ray diffraction (XRD) analysis of the films was conducted by simple modification of a conventional powder XRD diffractometer (Cu $K_\alpha$), where a lead foil was used as a mask to cover the whole disk with only one sample spot exposed at a time.

## 5.3 Results and Discussion

*Test of Concept*

The initial experiments were carried out to test the effectiveness of sealing and the effect of substrate orientation. Fig. 2 displays a 21-member array of zeolite films prepared using identical composition in all wells (0.15TPABr: 0.7NaOH: $98H_2O$) with the substrate held in the vertical position. Also shown is one member of the array under higher magnification. The figure indicates that the sealing was effective in confining the hydrothermal reaction inside each of the reaction wells. The sample film shown in Fig. 2 is circular and of uniform appearance, confirming that the substrate surface covered by the well was uniformly wetted despite the incomplete filling of the well. A simple experiment conducted at room temperature showed that the liquid assumes the configuration of Fig. 3a in preference to the alternative shown in Fig. 3c, evidently due to a lower surface energy as against the gravity potential at such a small volume.

Another issue of interest is whether the reduced solution volume is sufficient for the growth of zeolite films of morphology similar to that produced under conventional conditions. In the present experiments, the ratio of solution volume to substrate surface was ca. 0.5 cm, less than one-tenth of the ratio 5-20 cm used previously in our laboratory for zeolite film synthesis [12,13,22]. The zeolite films shown in Fig. 2 had thickness ca. 5 μm, and were well crystallized. They displayed morphology similar to that of films prepared conventionally from the same composition on porous or dense alumnina but in larger autoclaves using 10-150 mL solution [12]. On the other hand, the X-ray diffraction pattern of the films prepared by parallel synthesis differs somewhat from the pattern of the conventionally grown films in relative peak intensities, indicating lesser orientation of crystallites in the films grown in the wells. Preferred orientation of seeded growth is known to result from competitive growth of the fastest growing crystallographic axis, usually the c-axis [20,21], and depends on the extent of film growth. The lesser orientation of the films grown in the wells is then consistent with the lower volume to surface ratio of the wells.

Substrate orientation had an obvious effect on zeolite film morphology. Fig. 4 shows a ZSM-5 film prepared by placing the substrate horizontally at the bottom of the solution during parallel synthesis under otherwise identical conditions to those of Fig. 2. While the vertical synthesis geometry yielded a smooth and well-intergrown film, the horizontal geometry produced a continuous film with larger embedded particles, evidently as a result of precipitation of homogeneously grown crystals. At the larger volume-to-surface ratios used in standard autoclaves, precipitation of homogeneously

grown species is more extensive when the substrate is placed at the bottom of the solution [12].

***Parallel Synthesis from Clear, Organic-Free Solutions***

Exploration of clear, organic-free solutions for ZSM-5 film growth in the range $SiO_2$: xNaOH: $yAl_2O_3$: $80H_2O$ by parallel synthesis using 20 different compositions is summarized in Fig. 5. As expected, alkalinity was the major factor in the formation of a clear solution and for $NaOH/SiO_2 \geq 0.5$ the solutions were clear. The figure indicates that NaOH was also the most important factor affecting film morphology and $NaOH/SiO_2<0.8$ was required to form a continuous film. Interestingly, within the composition space $0.5 \leq NaOH/SiO_2 \leq 0.7$ and $300 \leq SiO_2/Al_2O_3 \leq 700$ the film morphology appeared insensitive to solution composition. Energy dispersive spectroscopy (EDS) of elemental composition gave for all films the estimate Si/Al~20, close to the lower bound allowed for ZSM-5. This ratio is much lower than the ratio Si/Al=150-350 in the solution, indicating that predominantly aluminum-rich species are involved in the growth of the ZSM-5 crystals in the absence of $TPA^+$ templates. The Si/Al ratio of these films is comparable to the Si/Al~15 ratio of ZSM-5 membranes prepared using $TPA^+$-free hydrogels [34], and much lower than the ratio Si/Al=100-200 often obtained for ZSM-5 films prepared using $TPA^+$ templates.

ZSM-5 films were also prepared conventionally from 10 mL solution to compare with the films synthesized in parallel. Fig. 6 shows a conventionally grown film, displaying morphology similar to that obtained by parallel synthesis. Additional films

were prepared conventionally varying $SiO_2/Al_2O_3$ ratios in the synthesis solution from 200 to 600. There was little effect of the $SiO_2/Al_2O_3$ ratio on morphology. The X-ray diffraction patterns of films grown in parallel and conventionally had some small differences as noted previously.

## 5.4 Conclusion

Parallel synthesis of ZSM-5 zeolite films was demonstrated using a 21-well reactor. Holding the substrate vertically provided uniform wetting of the substrate in the well area and favored heterogeneous film growth. The films prepared by parallel synthesis were shown to have similar morphology to those synthesized under conventional conditions but their X-ray diffraction patterns showed a more random orientation. Parallel synthesis was used to screen the composition space of organic-free clear synthesis solution for ZSM-5 film growth. The composition $SiO_2$: (0.5-0.7)NaOH: (1/300-1/700)$Al_2O_3$: 80$H_2O$ resulted in continuous ZSM-5 films of Si/Al~20.

## References

[1] Schultz, P.G.; Xiang, X.D. *Curr. Opin. Solid State Mat. Sci.* **1998**, *3*, 153.

[2] Bein, T. *Angew. Chem.-Int. Edit.* **1999**, *38*, 323.

[3] Engstrom, J.R.; Weinberg, W.H. *Aiche J.* **2000**, *46*, 2.

[4] Danielson, E.; Golden, J.H.; McFarland, E.W.; Reaves, C.M.; Weinberg, W.H.; Wu, X.D. *Nature* **1997**, *389*, 944.

[5] Xiang, X.D.; Sun, X.D.; Briceno, G.; Lou, Y.L.; Wang, K.A.; Chang, H.Y.; Wallacefreedman, W.G.; Chen, S.W.; Schultz, P.G. *Science* **1995**, *268*, 1738.

[6] Chang, H.; Takeuchi, I.; Xiang, X.D. *Appl. Phys. Lett.* **1999**, *74*, 1165.

[7] Taylor, S.J.; Morken, J.P. *Science* **1998**, *280*, 267.

[8] Holzwarth, A.; Schmidt, P.W.; Maier, W.E. *Angew. Chem.-Int. Edit.* **1998**, *37*, 2644.

[9] Senkan, S.M. *Nature* **1998**, *394*, 350.

[10] Cong, P.J.; Doolen, R.D.; Fan, Q.; Giaquinta, D.M.; Guan, S.H.; McFarland, E.W.; Poojary, D.M.; Self, K.; Turner, H.W.; Weinberg, W.H. *Angew. Chem.-Int. Edit.* **1999**, *38*, 483.

[11] Hoffmann, C.; Wolf, A.; Schuth, F. *Angew. Chem.-Int. Edit.* **1999**, *38*, 2800.

[12] Lai, R.; Gavalas, G.R. *Ind. Eng. Chem. Res.* **1998**, *37*, 4275.

[13] Yan, Y.S.; Davis, M.E.; Gavalas, G.R. *Ind. Eng. Chem. Res.* **1995**, *34*, 1652.

[14] Geus, E.R.; den Exter, M.J.; van Bekkum, H. *J. Chem. Soc.-Faraday Trans.* **1992**, *88*, 3101.

[15] Coronas, J.; Falconer, J.L.; Noble, R.D. *AICHE J.* **1997**, *43*, 1797.

[16] Vroon, Z.; Keizer, K.; Burggraaf, A.J.; Verweij, H. *J. Membr. Sci.* **1998**, *144*, 65.

[17] Lovallo, M.C.; Gouzinis, A.; Tsapatsis, M. *AICHE J.* **1998**, *44*, 1903.

[18] Bein, T. *Chem. Mat.* **1996**, *8*, 1636.

[19] Koegler, J.H.; Zandbergen, H.W.; Harteveld, J.L.N.; Nieuwenhuizen, M.S.; Jansen, J.C.; van Bekkum, H. *Stud. Surf. Sci. Catal.* **1994**, *84*, 307.

[20] Lovallo, M.C.; Tsapatsis, M. *AICHE J.* **1996**, *42*, 3020.

[21] Gouzinis, A.; Tsapatsis, M. *Chem. Mat.* **1998**, *10*, 2497.

[22] Lai, R.; Yan, Y.; Gavalas, G.R. *Micropor. Mesopor. Mat.* **2000**, *37*, 9.

[23] Akporiaye, D.E.; Dahl, I.M.; Karlsson, A.; Wendelbo, R. *Angew. Chem.-Int. Edit.* **1998**, *37*, 609.

[24] Klein, J.; Lehmann, C.W.; Schmidt, H.W.; Maier, W.F. *Angew. Chem.-Int. Edit.* **1998**, *37*, 3369.

[25] Choi, K.; Gardner, D.; Hilbrandt, N.; Bein, T. *Angew. Chem.-Int. Edit.* **1999**, *38*, 2891.

[26] Orschel, M.; Klein, J.; Schmidt, H.W.; Maier, W.F. *Angew. Chem.-Int. Edit.* **1999**, *38*, 2791.

[27] Geus, E.R.; Van Bekkum, H. *Zeolites* **1995**, *15*, 333.

[28] den Exter, M.J.; van Bekkum, H.; Rijn, C.J.M.; Kapteijn, F.; Moulijn, J.A.; Schellevis, H.; Beenakker, C.I.N. *Zeolites* **1997**, *19*, 13.

[29] Lin, X.; Falconer, J.L.; Noble, R.D. *Chem. Mat.* **1998**, *10*, 3716.

[30] Dong, J.H.; Lin, Y.S.; Hu, M.Z.C.; Peascoe, R.A.; Payzant, E.A. *Microporous Mesoporous Mat.* **2000**, *34*, 241.

[31] Aiello, R.; Crea, F.; Nastro, A.; Pellegrino, C. *Zeolites* **1987**, *7*, 549.

[32] Shiralkar, V.P.; Clearfield, A. *Zeolites* **1989**, *9*, 363.

[33] Schwieger, W.; Bergk, K.-H.; Freude, D.; Hunger, M.; Pfeifer, H. In *Zeolite Synthesis*, Occelli, M.L. and Robson, H.E., Ed.; ACS: Washington, D.C., 1989; p. 274.

[34] Lai, R.; Gavalas, G.R. *Micropor. Mesopor. Mat.* **2000** (in print).

[35] Kern, W.; Puotinen, D.A. *RCA Reviews* **1970**, *31*, 187.

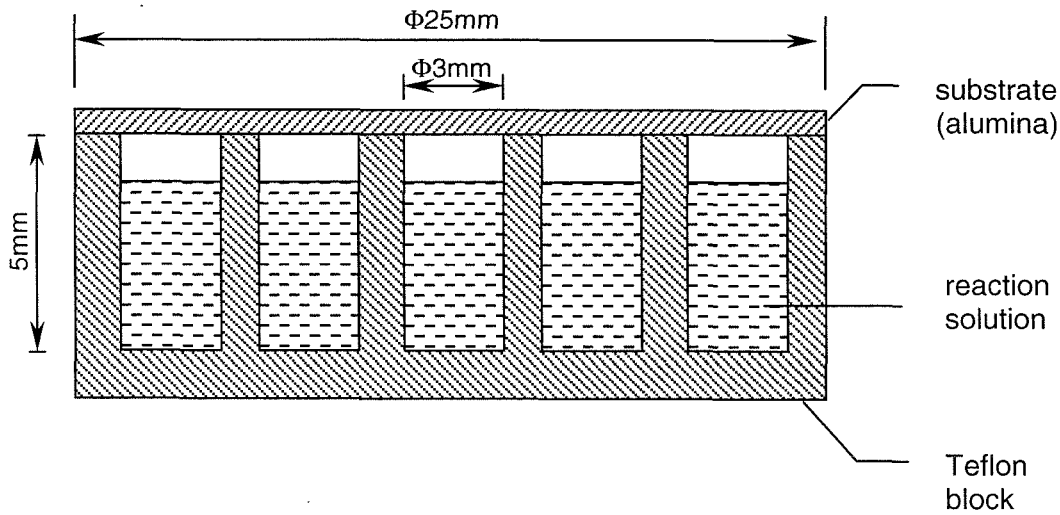


**Figure 5-1** Cross section of the multi-well reactor.

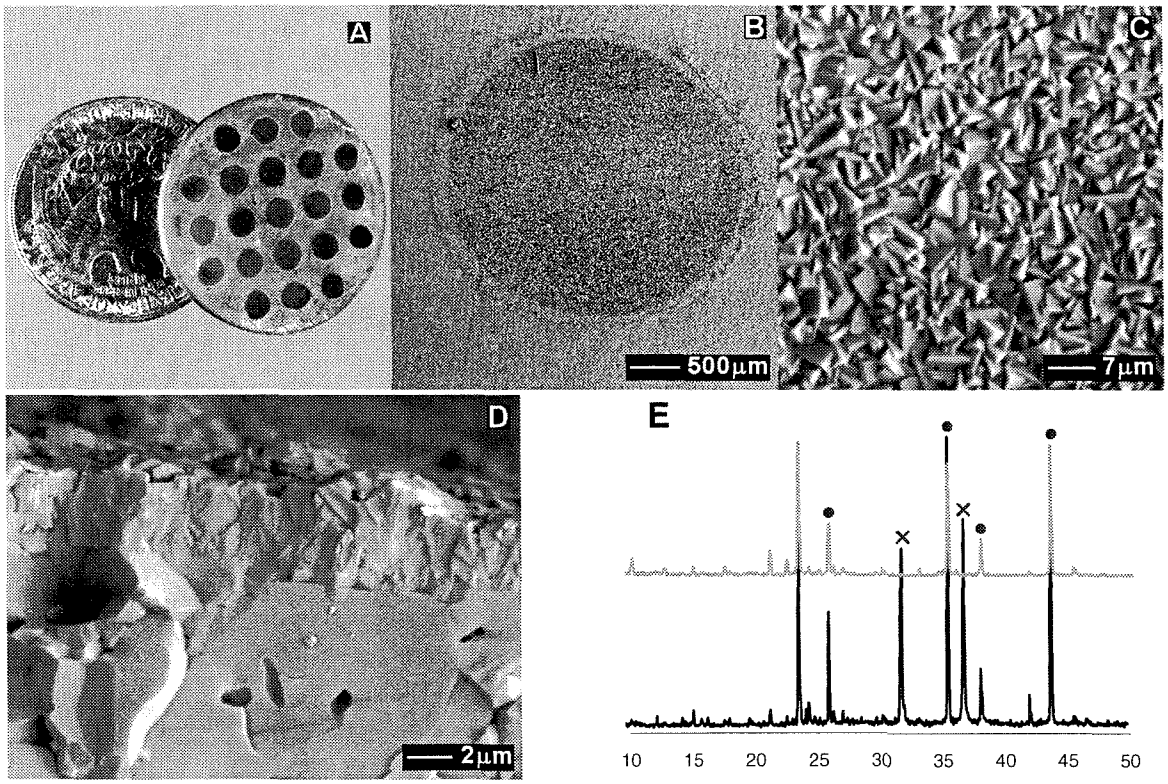


**Figure 5-2** An array of ZSM-5 zeolite films on an alumina disk. The hydrothermal reaction was carried out on a seeded alumina disk for 16 h at 150°C with the substrate held vertically during the synthesis. (A) The 21-member array disk, displayed with a quarter coin in the background. (B, C) A sample spot in the array under magnification. (D) SEM of a film cross section. (E) X-ray diffraction patterns of a sample spot in the array (bottom) and a conventionally grown film (top). The dots mark peaks from the alumina substrate, and the crosses mark peaks from the lead mask.

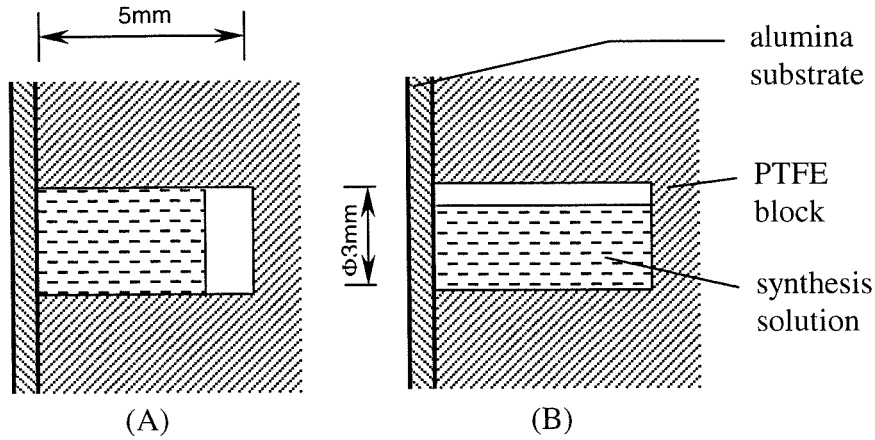


**Figure 5-3** Liquid position for the vertically oriented substrate. (A) Horizontal solution column formed following the adopted loading procedure. (B) Position not realized.

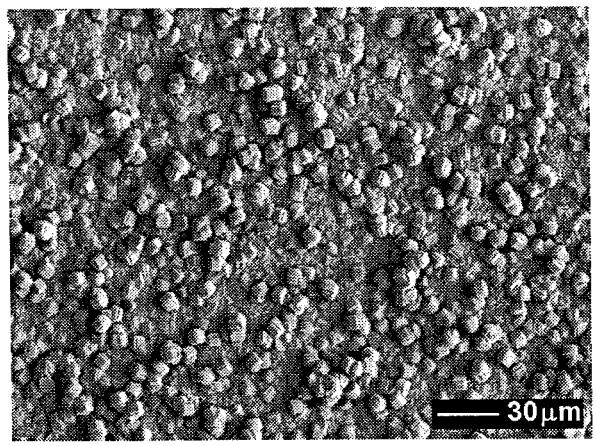


**Figure 5-4** ZSM-5 film prepared with the seeded alumina disk placed at the bottom of the solution.

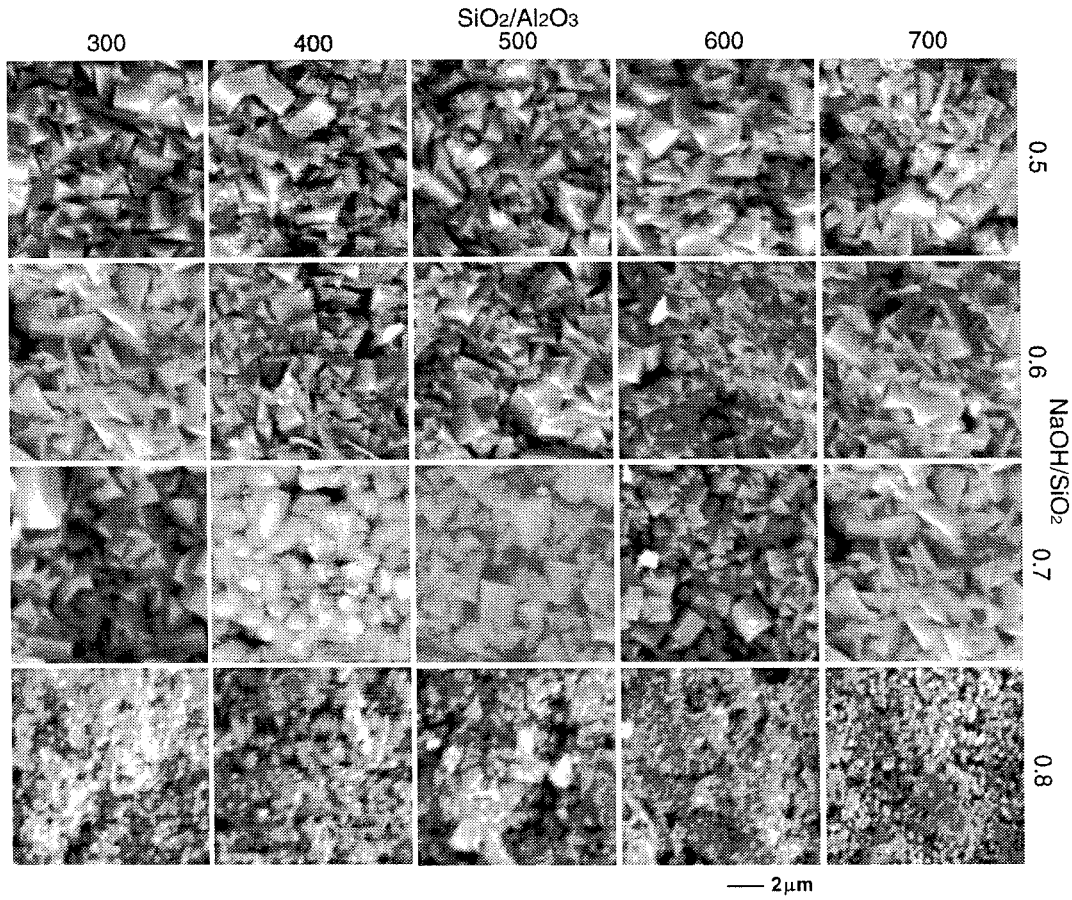


**Figure 5-5** ZSM-5 films prepared from clear synthesis solutions of composition $SiO_2$: $x$NaOH: $y$$Al_2O_3$: 80$H_2O$. The reaction was carried out at 180°C for 16 h on a seeded alumina disk held vertically.

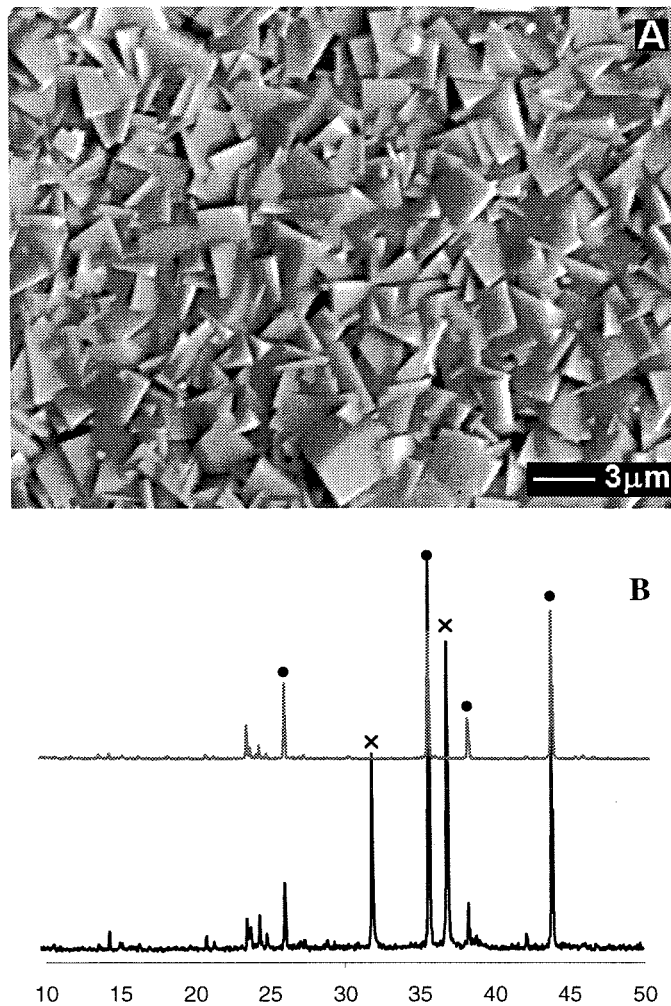


**Figure 5-6** (A) SEM micrograph of a ZSM-5 film prepared conventionally on a seeded alumina substrate placed in a 10 mL reactor. The reaction was carried out for 16 h at 180°C in a clear solution of composition $SiO_2$: 0.5NaOH: 1/300 $Al_2O_3$: $80H_2O$. (B) X-ray diffraction pattern of the film (top curve), compared with that of a film prepared by parallel synthesis (bottom curve). The peaks marked with a dot originate from the alumina substrate, and the peaks marked with a cross from the lead mask.

**Chapter 6**

# Conclusions

In-situ growth of supported ZSM-5 zeolite films under strongly alkaline compositions is mediated by formation of a precursor gel layer on the support. Subsequent zeolite crystallization occurs inside the gel layer. Supports having a high Hammaker constant and the presence of aluminates are identified as necessary for the formation of the layer for certain compositions. Aluminate ions added to the synthesis mixture or leached from the substrate have dual roles in the film growth, to facilitate the formation of the gel layer on the support and to retard crystallization in this gel layer as well as crystallization in the bulk solution. As a result, zeolite membrane synthesis is sensitive to the choice of alumina substrates owing to their different dissolution rates.

A synthesis strategy based on surface seeding was developed for reliable and robust ZSM-5 membrane synthesis. Use of supports coated with a dense layer of zeolite particles eliminates the requirement of surface nucleation. Zeolite films can grow on seeded substrates at lower temperatures and shorter times than required when using unseeded supports. Enlargement of window of crystallization by surface seeding allows to eliminate the structure-directing agent $TPA^+$ from the synthesis mixture, and, therefore, the crack-prone calcination used to remove encapsulated $TPA^+$ from the as-synthesized ZSM-5. The resultant membranes displayed selectivities of $H_2$ over $N_2$ as large as 500 and $H_2$ over n-butane beyond $10^4$ at room temperature.

An interesting issue for supported zeolite membrane synthesis is that aluminosilicate materials form on top as well as inside the pores of the substrate. The external layer appears crystalline based on cross-section SEM examination, but the nature of the internal layer is largely unclear. Gas adsorption was applied in this study to

characterize these materials. In particular, we used the steps on the Ar and iso-butane isotherms corresponding to adsorbate "phase" transition inside ZSM-5 zeolite that is characteristic of both the adsorbent and the adsorbate. The crystallinity of the aluminosilicates formed on macroporous alumina supports, with or without surface seeding, was found to be 40-50%. The amorphous materials did not contribute to the gas adsorptions in the micropore regime, and probably added significantly to the resistance to permeation. Elimination of these materials would be desirable in future work.

As zeolite membrane synthesis usually starts with a tedious period of trial and error to identify the synthesis compositions that lead to microscopically continuous and intergrown films, parallel synthesis of ZSM-5 zeolite films was developed to expedite composition screening. The films were shown to have similar morphology to those synthesized under conventional conditions, but had slightly different preferred crystallographic orientation. Parallel synthesis was used to screen the composition space of clear, organic-free synthesis solution for ZSM-5 film growth.